

Hybrid Textures of Majorana Neutrino Mass Matrix and Current Experimental Tests

Ji-Yuan Liu ^{*}

College of Science, Tianjin University of Technology, Tianjin 300384, China

Shun Zhou [†]

*Department of Theoretical Physics, School of Engineering Sciences,
KTH Royal Institute of Technology, 106 91 Stockholm, Sweden*

Abstract

Motivated by recent measurements of a relatively large θ_{13} in the Daya Bay and RENO reactor neutrino experiments, we carry out a systematic analysis of the hybrid textures of Majorana neutrino mass matrix M_ν , which contain one texture zero and two equal nonzero matrix elements. We show that three neutrino masses (m_1, m_2, m_3) and three leptonic CP-violating phases (δ, ρ, σ) can fully be determined from two neutrino mass-squared differences ($\delta m^2, \Delta m^2$) and three flavor mixing angles ($\theta_{12}, \theta_{23}, \theta_{13}$). Out of sixty logically possible patterns of M_ν , thirty-nine are found to be compatible with current experimental data at the 3σ level. We demonstrate that the texture zero of M_ν is stable against one-loop quantum corrections, while the equality between two independent elements not. Phenomenological implications of M_ν for the neutrinoless double-beta decay and leptonic CP violation are discussed, and a realization of the texture zero and equality by means of discrete flavor symmetries is illustrated.

PACS numbers: 14.60.Lm, 14.60.Pq

^{*}E-mail: liujy@tjut.edu.cn

[†]E-mail: shunzhou@kth.se

1 Introduction

Recent years have seen great progress in neutrino physics [1]. Thanks to a number of elegant solar, atmospheric, accelerator and reactor neutrino oscillation experiments [2], two neutrino mixing angles are found to be quite large (i.e., $\theta_{12} \approx 34^\circ$ and $\theta_{23} \approx 40^\circ$), while two independent neutrino mass-squared differences $\delta m^2 \equiv m_2^2 - m_1^2$ and $\Delta m^2 \equiv m_3^2 - (m_1^2 + m_2^2)/2$ are measured with a good degree of accuracy (i.e., $\delta m^2 \approx 7.5 \times 10^{-5} \text{ eV}^2$ and $|\Delta m^2| \approx 2.5 \times 10^{-3} \text{ eV}^2$). The latest results from the Daya Bay [3] and RENO [4] experiments reveal that $\theta_{13} \approx 9^\circ$ is relatively large, which is very crucial to determine the neutrino mass hierarchy (i.e., the sign of Δm^2) and to discover the leptonic CP violation (i.e., the Dirac CP-violating phase δ) in the future long-baseline neutrino oscillation experiments. However, the absolute scale of neutrino masses and whether neutrinos are Dirac or Majorana particles are still unknown.

On the theoretical side, a satisfactory description of tiny neutrino masses and leptonic mixing pattern is still lacking. Although the seesaw mechanisms can be responsible for the generation of light neutrino masses [5, 6, 7], they leave the lepton flavor structure intact. In fact, it was shown one decade ago that the large leptonic mixing can be achieved by taking two independent elements of Majorana neutrino mass matrix M_ν to be zero, in the flavor basis where the charged-lepton mass matrix M_l is diagonal [8, 9, 10, 11]. Recently, several authors have demonstrated that these seven two-zero textures of M_ν still survive the current neutrino oscillation data [12, 13]. Furthermore, it has been pointed out that those texture zeros can be realized by implementing the Z_n flavor symmetry in the type-II seesaw model, where the Higgs triplets are introduced to account for tiny Majorana neutrino masses [12]. Apart from texture zeros in the neutrino mass matrix, possible correlations between two matrix elements of M_ν have recently been investigated [14].

In the present paper, we perform a systematic study of M_ν with one texture zero and two equal nonzero elements, which has been termed as “hybrid texture” in the literature [15, 16, 17]. The motivation for such an investigation is three-fold. First, from the phenomenological point of view, either one texture zero or an equality between two independent entries in M_ν imposes one constraint condition and thus reduces the number of real free model parameters by two. Hence the hybrid textures are as predictive as the well-known two-zero textures, and deserve a detailed analysis. See, e.g., Refs. [15] and [16], for previous studies of hybrid textures. The textures with two equalities and other phenomenological assumptions have also been considered [18, 19]. Second, it has been proved that a texture zero in any position in M_ν can be realized by using Abelian flavor symmetries Z_n [20, 21] or $U(1)$ [22]. However, the equality between two nonzero matrix elements should come from a non-Abelian flavor symmetry. Third, now that a good knowledge about three neutrino mixing angles and two neutrino mass-squared differences has been obtained, it is timely to reexamine the possible structure of M_ν and explore the underlying symmetry in the lepton sector. Taking into account current neutrino oscillation data at the 3σ level, we have found that thirty-nine out of sixty logically possible hybrid textures of M_ν are viable. If the 1σ ranges of neutrino mixing parameters are considered, only thirteen hybrid textures can survive.

The remaining part of our paper is organized as follows. In section 2, we introduce the hybrid textures and present some useful analytical formulas. Then, the stability of texture zeros and equalities in M_ν against quantum corrections is briefly discussed by using the one-loop renormalization group equation. Section 3 is devoted to the analytical analysis of six viable patterns, which serve as typical examples of hybrid textures. We show that three neutrino masses (m_1, m_2, m_3) and three CP-violating phases (δ, ρ, σ) can fully be determined from neutrino mixing angles $(\theta_{12}, \theta_{23}, \theta_{13})$ and neutrino mass-squared differences $(\delta m^2, \Delta m^2)$. In section 4, a thorough numerical analysis has been performed, and the allowed parameter space of the chosen six viable patterns is given. To illustrate how to realize a hybrid texture, we give a concrete example in section 5, where a type-II seesaw model with an $S_3 \otimes Z_3$ flavor symmetry is considered. Finally, we summarize our main conclusions in section 6.

2 Hybrid Textures

2.1 Classification

At low energies, lepton mass spectra and flavor mixing are determined by the charged-lepton mass matrix M_l and the effective neutrino mass matrix M_ν . We assume massive neutrinos to be Majorana particles, as in various seesaw models [5, 6, 7], so M_ν is in general a 3×3 symmetric complex matrix. If one of six independent matrix elements of M_ν is taken to be zero and two of the rest are equal, we finally arrive at $C_6^1 \cdot C_5^2 = 60$ logically possible textures.

We enumerate all the 39 hybrid textures, which are compatible with current neutrino oscillation data at the 3σ level and can be classified into six categories:

$$\mathbf{A}_1 : \begin{pmatrix} 0 & \times & \times \\ \times & \triangle & \triangle \\ \times & \triangle & \times \end{pmatrix}, \quad \mathbf{A}_2 : \begin{pmatrix} 0 & \times & \times \\ \times & \triangle & \times \\ \times & \times & \triangle \end{pmatrix}, \quad \mathbf{A}_3 : \begin{pmatrix} 0 & \times & \times \\ \times & \times & \triangle \\ \times & \triangle & \triangle \end{pmatrix}; \quad (1)$$

$$\begin{aligned} \mathbf{B}_1 : \begin{pmatrix} \triangle & 0 & \triangle \\ 0 & \times & \times \\ \triangle & \times & \times \end{pmatrix}, \quad \mathbf{B}_2 : \begin{pmatrix} \times & 0 & \triangle \\ 0 & \triangle & \times \\ \triangle & \times & \times \end{pmatrix}, \quad \mathbf{B}_3 : \begin{pmatrix} \times & 0 & \triangle \\ 0 & \times & \times \\ \triangle & \times & \triangle \end{pmatrix}, \\ \mathbf{B}_4 : \begin{pmatrix} \times & 0 & \times \\ 0 & \triangle & \triangle \\ \times & \triangle & \times \end{pmatrix}, \quad \mathbf{B}_5 : \begin{pmatrix} \times & 0 & \times \\ 0 & \times & \triangle \\ \times & \triangle & \triangle \end{pmatrix}; \end{aligned} \quad (2)$$

$$\begin{aligned} \mathbf{C}_1 : \begin{pmatrix} \triangle & \triangle & 0 \\ \triangle & \times & \times \\ 0 & \times & \times \end{pmatrix}, \quad \mathbf{C}_2 : \begin{pmatrix} \times & \triangle & 0 \\ \triangle & \triangle & \times \\ 0 & \times & \times \end{pmatrix}, \quad \mathbf{C}_3 : \begin{pmatrix} \times & \triangle & 0 \\ \triangle & \times & \times \\ 0 & \times & \triangle \end{pmatrix}, \\ \mathbf{C}_4 : \begin{pmatrix} \times & \times & 0 \\ \times & \triangle & \triangle \\ 0 & \triangle & \times \end{pmatrix}, \quad \mathbf{C}_5 : \begin{pmatrix} \times & \times & 0 \\ \times & \times & \triangle \\ 0 & \triangle & \triangle \end{pmatrix}; \end{aligned} \quad (3)$$

$$\begin{aligned}
\mathbf{D}_1 &: \begin{pmatrix} \triangle & \triangle & \times \\ \triangle & \times & 0 \\ \times & 0 & \times \end{pmatrix}, & \mathbf{D}_2 &: \begin{pmatrix} \triangle & \times & \triangle \\ \times & \times & 0 \\ \triangle & 0 & \times \end{pmatrix}, & \mathbf{D}_3 &: \begin{pmatrix} \times & \triangle & \times \\ \triangle & \triangle & 0 \\ \times & 0 & \times \end{pmatrix}, \\
\mathbf{D}_4 &: \begin{pmatrix} \times & \triangle & \times \\ \triangle & \times & 0 \\ \times & 0 & \triangle \end{pmatrix}, & \mathbf{D}_5 &: \begin{pmatrix} \times & \times & \triangle \\ \times & \triangle & 0 \\ \triangle & 0 & \times \end{pmatrix}, & \mathbf{D}_6 &: \begin{pmatrix} \times & \times & \triangle \\ \times & \times & 0 \\ \triangle & 0 & \triangle \end{pmatrix}; \quad (4)
\end{aligned}$$

$$\begin{aligned}
\mathbf{E}_1 &: \begin{pmatrix} \triangle & \triangle & \times \\ \triangle & 0 & \times \\ \times & \times & \times \end{pmatrix}, & \mathbf{E}_2 &: \begin{pmatrix} \triangle & \times & \triangle \\ \times & 0 & \times \\ \triangle & \times & \times \end{pmatrix}, & \mathbf{E}_3 &: \begin{pmatrix} \triangle & \times & \times \\ \times & 0 & \triangle \\ \times & \triangle & \times \end{pmatrix}, & \mathbf{E}_4 &: \begin{pmatrix} \triangle & \times & \times \\ \times & 0 & \times \\ \times & \times & \triangle \end{pmatrix}, \\
\mathbf{E}_5 &: \begin{pmatrix} \times & \triangle & \triangle \\ \triangle & 0 & \times \\ \triangle & \times & \times \end{pmatrix}, & \mathbf{E}_6 &: \begin{pmatrix} \times & \triangle & \times \\ \triangle & 0 & \triangle \\ \times & \triangle & \times \end{pmatrix}, & \mathbf{E}_7 &: \begin{pmatrix} \times & \triangle & \times \\ \triangle & 0 & \times \\ \times & \times & \triangle \end{pmatrix}, & \mathbf{E}_8 &: \begin{pmatrix} \times & \times & \triangle \\ \times & 0 & \triangle \\ \triangle & \triangle & \times \end{pmatrix}, \\
\mathbf{E}_9 &: \begin{pmatrix} \times & \times & \triangle \\ \times & 0 & \times \\ \triangle & \times & \triangle \end{pmatrix}, & \mathbf{E}_{10} &: \begin{pmatrix} \times & \times & \times \\ \times & 0 & \triangle \\ \times & \triangle & \triangle \end{pmatrix}; \quad (5)
\end{aligned}$$

$$\begin{aligned}
\mathbf{F}_1 &: \begin{pmatrix} \triangle & \triangle & \times \\ \triangle & \times & \times \\ \times & \times & 0 \end{pmatrix}, & \mathbf{F}_2 &: \begin{pmatrix} \triangle & \times & \triangle \\ \times & \times & \times \\ \triangle & \times & 0 \end{pmatrix}, & \mathbf{F}_3 &: \begin{pmatrix} \triangle & \times & \times \\ \times & \triangle & \times \\ \times & \times & 0 \end{pmatrix}, & \mathbf{F}_4 &: \begin{pmatrix} \triangle & \times & \times \\ \times & \times & \triangle \\ \times & \triangle & 0 \end{pmatrix}, \\
\mathbf{F}_5 &: \begin{pmatrix} \times & \triangle & \triangle \\ \triangle & \times & \times \\ \triangle & \times & 0 \end{pmatrix}, & \mathbf{F}_6 &: \begin{pmatrix} \times & \triangle & \times \\ \triangle & \triangle & \times \\ \times & \times & 0 \end{pmatrix}, & \mathbf{F}_7 &: \begin{pmatrix} \times & \triangle & \times \\ \triangle & \times & \triangle \\ \times & \triangle & 0 \end{pmatrix}, & \mathbf{F}_8 &: \begin{pmatrix} \times & \times & \triangle \\ \times & \triangle & \times \\ \triangle & \times & 0 \end{pmatrix}, \\
\mathbf{F}_9 &: \begin{pmatrix} \times & \times & \triangle \\ \times & \times & \triangle \\ \triangle & \triangle & 0 \end{pmatrix}, & \mathbf{F}_{10} &: \begin{pmatrix} \times & \times & \times \\ \times & \triangle & \triangle \\ \times & \triangle & 0 \end{pmatrix}, \quad (6)
\end{aligned}$$

where the triangles “ \triangle ” denote equal and nonzero elements, while the crosses “ \times ” stand for arbitrary and nonzero ones.

If one more element of M_ν is assumed to be zero (or two more elements are equal), the number of free parameters in M_ν will be further reduced and the viable textures should be much less (see, for example, Ref. [14]). However, we have numerically checked that all those textures have already been excluded by current neutrino oscillation data at the 3σ level.

2.2 Important Relations

In the basis where the charged-lepton mass matrix M_l is diagonal, the Majorana neutrino mass matrix M_ν can be reconstructed from the leptonic mixing matrix V and three neutrino masses:

$$M_\nu = V \begin{pmatrix} m_1 & 0 & 0 \\ 0 & m_2 & 0 \\ 0 & 0 & m_3 \end{pmatrix} V^T. \quad (7)$$

The leptonic mixing matrix can be parametrized as $V = U \cdot P$, where the unitary matrix U contains three mixing angles $(\theta_{12}, \theta_{23}, \theta_{13})$ and one Dirac-type CP-violating phase δ , namely,

$$U = \begin{pmatrix} c_{12}c_{13} & s_{12}c_{13} & s_{13} \\ -c_{12}s_{23}s_{13} - s_{12}c_{23}e^{-i\delta} & -s_{12}s_{23}s_{13} + c_{12}c_{23}e^{-i\delta} & s_{23}c_{13} \\ -c_{12}c_{23}s_{13} + s_{12}s_{23}e^{-i\delta} & -s_{12}c_{23}s_{13} - c_{12}s_{23}e^{-i\delta} & c_{23}c_{13} \end{pmatrix}; \quad (8)$$

and $P = \text{Diag}\{e^{i\rho}, e^{i\sigma}, 1\}$ is a diagonal matrix with ρ and σ being two Majorana-type CP-violating phases. Here we have defined $s_{ij} \equiv \sin \theta_{ij}$ and $c_{ij} \equiv \cos \theta_{ij}$ for $ij = 12, 23, 13$. For later convenience, we rewrite

$$M_\nu = U \begin{pmatrix} \lambda_1 & 0 & 0 \\ 0 & \lambda_2 & 0 \\ 0 & 0 & \lambda_3 \end{pmatrix} U^T, \quad (9)$$

where $\lambda_1 \equiv m_1 e^{2i\rho}$, $\lambda_2 \equiv m_2 e^{2i\sigma}$ and $\lambda_3 \equiv m_3$.

If one matrix element is zero [e.g., $(M_\nu)_{ab} = 0$] and two other elements are equal [e.g., $(M_\nu)_{\alpha\beta} = (M_\nu)_{cd}$], where three different independent elements of M_ν are considered, we obtain

$$\sum_{i=1}^3 U_{ai} U_{bi} \lambda_i = 0 \quad \text{and} \quad \sum_{i=1}^3 (U_{\alpha i} U_{\beta i} - U_{ci} U_{di}) \lambda_i = 0, \quad (10)$$

which lead to

$$\begin{aligned} \frac{\lambda_1}{\lambda_3} &= \frac{U_{a3} U_{b3} U_{\alpha 2} U_{\beta 2} - U_{a2} U_{b2} U_{\alpha 3} U_{\beta 3} + U_{a2} U_{b2} U_{c3} U_{d3} - U_{a3} U_{b3} U_{c2} U_{d2}}{U_{a2} U_{b2} U_{\alpha 1} U_{\beta 1} - U_{a1} U_{b1} U_{\alpha 2} U_{\beta 2} + U_{a1} U_{b1} U_{c2} U_{d2} - U_{a2} U_{b2} U_{c1} U_{d1}}, \\ \frac{\lambda_2}{\lambda_3} &= \frac{U_{a1} U_{b1} U_{\alpha 3} U_{\beta 3} - U_{a3} U_{b3} U_{\alpha 1} U_{\beta 1} + U_{a3} U_{b3} U_{c1} U_{d1} - U_{a1} U_{b1} U_{c3} U_{d3}}{U_{a2} U_{b2} U_{\alpha 1} U_{\beta 1} - U_{a1} U_{b1} U_{\alpha 2} U_{\beta 2} + U_{a1} U_{b1} U_{c2} U_{d2} - U_{a2} U_{b2} U_{c1} U_{d1}}. \end{aligned} \quad (11)$$

With the help of Eq. (11), one can figure out two neutrino mass ratios $\xi \equiv m_1/m_3 = |\lambda_1/\lambda_3|$ and $\zeta \equiv m_2/m_3 = |\lambda_2/\lambda_3|$, as well as two Majorana CP-violating phases $\rho = \arg[\lambda_1/\lambda_3]/2$ and $\sigma = \arg[\lambda_2/\lambda_3]/2$. As we shall show later, these important relations are quite useful in the determination of both neutrino mass spectrum and leptonic CP-violating phases from current experimental observations.

If both $(\theta_{12}, \theta_{23}, \theta_{13})$ and δ are precisely measured in neutrino oscillation experiments, the unitary matrix U is fixed, thus both (ξ, ζ) and (ρ, σ) can be determined from Eq. (11). The neutrino mass ratios ξ and ζ are related to the ratio of two independent neutrino mass-squared differences as

$$R_\nu \equiv \frac{\delta m^2}{|\Delta m^2|} = \frac{2(\zeta^2 - \xi^2)}{|2 - (\zeta^2 + \xi^2)|}, \quad (12)$$

and to three neutrino masses as

$$m_3 = \sqrt{\frac{\delta m^2}{\zeta^2 - \xi^2}}, \quad m_2 = m_3 \zeta, \quad m_1 = m_3 \xi. \quad (13)$$

At present, the CP-violating phase δ is essentially unconstrained in neutrino oscillation experiments. If one of the hybrid textures is assumed, and three neutrino mixing angles and two

Table 1: The latest global-fit results of three neutrino mixing angles ($\theta_{12}, \theta_{23}, \theta_{13}$) and two neutrino mass-squared differences $\delta m^2 \equiv m_2^2 - m_1^2$ and $\Delta m^2 \equiv m_3^2 - (m_1^2 + m_2^2)/2$ in the case of normal neutrino mass hierarchy [23].

Parameter	δm^2 (10^{-5} eV ²)	Δm^2 (10^{-3} eV ²)	θ_{12}	θ_{23}	θ_{13}
Best fit	7.54	2.43	33.6°	38.4°	8.9°
1 σ range	[7.32, 7.80]	[2.33, 2.49]	[32.6°, 34.8°]	[37.2°, 40.0°]	[8.5°, 9.4°]
2 σ range	[7.15, 8.00]	[2.27, 2.55]	[31.6°, 35.8°]	[36.2°, 42.0°]	[8.0°, 9.8°]
3 σ range	[6.99, 8.18]	[2.19, 2.62]	[30.6°, 36.8°]	[35.1°, 53.0°]	[7.5°, 10.2°]

neutrino mass-squared differences are given, then δ can be predicted from Eq. (12). For the normal neutrino mass hierarchy, the latest global-fit analysis yields at the 3 σ level [23]

$$\begin{aligned}
0.259 &\leq \sin^2 \theta_{12} \leq 0.359 , \\
0.331 &\leq \sin^2 \theta_{23} \leq 0.637 , \\
0.017 &\leq \sin^2 \theta_{13} \leq 0.031 ,
\end{aligned} \tag{14}$$

and

$$\begin{aligned}
6.99 \times 10^{-5} \text{ eV}^2 &\leq \delta m^2 \leq 8.18 \times 10^{-5} \text{ eV}^2 , \\
2.19 \times 10^{-3} \text{ eV}^2 &\leq \Delta m^2 \leq 2.62 \times 10^{-3} \text{ eV}^2 .
\end{aligned} \tag{15}$$

For the inverted neutrino mass hierarchy, the 3 σ ranges of neutrino mixing angles and mass-squared differences are slightly different, so we shall use the same values as in the case of normal neutrino mass hierarchy. In Table 1, the best-fit values together with the 1 σ , 2 σ , and 3 σ ranges are summarized [‡].

2.3 Quantum Corrections

The stability of texture zeros in M_ν against radiative corrections has been extensively studied in the literature [12]. By using the one-loop renormalization group equation (RGE), one can demonstrate that the texture zeros in M_ν at a high-energy scale remain there at low-energy scales. In this subsection, we examine the stability of texture zeros and equality between two matrix elements against quantum corrections.

To be explicit, we consider the unique dimension-5 Weinberg operator of massive Majorana neutrinos in an effective field theory after the heavy degrees of freedom are integrated out [26]:

$$\frac{\mathcal{L}_{\text{d=5}}}{\Lambda} = \frac{1}{2} \kappa_{\alpha\beta} \overline{\ell_{\alpha\text{L}}} \tilde{H} \tilde{H}^T \ell_{\beta\text{L}}^c + \text{h.c.} , \tag{16}$$

[‡]The global-fit analysis of current neutrino oscillation experiments has also been performed by two other groups [24, 25]. Although their best-fit results of three flavor mixing angles are slightly different from those obtained in Ref. [23], such differences become insignificant at the 3 σ level.

where Λ is the cutoff scale, ℓ_L denotes the left-handed lepton doublet, $\tilde{H} \equiv i\sigma_2 H^*$ with H being the standard-model Higgs doublet, and κ stands for the effective neutrino coupling matrix. After spontaneous gauge symmetry breaking, \tilde{H} gains its vacuum expectation value $\langle \tilde{H} \rangle = v/\sqrt{2}$ with $v \approx 246$ GeV. We are then left with the effective Majorana mass matrix $M_\nu = \kappa v^2/2$ for three light neutrinos from Eq. (16). If the dimension-5 Weinberg operator is obtained in the framework of the minimal supersymmetric standard model, one will be left with $M_\nu = \kappa(v \sin \beta)^2/2$, where $\tan \beta$ denotes the ratio of the vacuum expectation values of two Higgs doublets. Eq. (16) or its supersymmetric counterpart can provide a simple but generic way of generating tiny neutrino masses. There are a number of interesting possibilities of building renormalizable gauge models to realize the effective Weinberg mass operator, such as the well-known seesaw mechanisms at a superhigh energy scale Λ [5, 6, 7].

The running of M_ν from Λ to the electroweak scale $\mu \simeq M_Z$ (or vice versa) is described by the RGE's [27]. In the chosen flavor basis and at the one-loop level, $M_\nu(M_Z)$ and $M_\nu(\Lambda)$ are related to each other via

$$M_\nu(M_Z) = I_0 \begin{pmatrix} I_e & 0 & 0 \\ 0 & I_\mu & 0 \\ 0 & 0 & I_\tau \end{pmatrix} M_\nu(\Lambda) \begin{pmatrix} I_e & 0 & 0 \\ 0 & I_\mu & 0 \\ 0 & 0 & I_\tau \end{pmatrix}, \quad (17)$$

where the RGE evolution function I_0 denotes the overall contribution from gauge and quark Yukawa couplings, and I_α (for $\alpha = e, \mu, \tau$) stand for the contributions from charged-lepton Yukawa couplings [28]. Because of $I_e < I_\mu < I_\tau$ as a consequence of $m_e \ll m_\mu \ll m_\tau$, they can modify the texture of M_ν . In comparison, $I_0 \neq 1$ only affects the overall mass scale of M_ν . Note, however, that the texture zeros of M_ν are stable against such quantum corrections induced by the one-loop RGE's. Taking **Pattern A₁** of M_ν for example, we have

$$M_\nu^{\mathbf{A}_1}(\Lambda) = \begin{pmatrix} 0 & a & b \\ a & d & d \\ b & d & c \end{pmatrix} \quad (18)$$

at Λ , and thus

$$M_\nu^{\mathbf{A}_1}(M_Z) = I_0 \begin{pmatrix} 0 & aI_e I_\mu & bI_e I_\tau \\ aI_e I_\mu & dI_\mu^2 & dI_\mu I_\tau \\ bI_e I_\tau & dI_\mu I_\tau & cI_\tau^2 \end{pmatrix} \quad (19)$$

at M_Z . Although the texture zero is stable, the equality $(M_\nu^{\mathbf{A}_1})_{\mu\mu} = (M_\nu^{\mathbf{A}_1})_{\mu\tau}$ at Λ is spoiled at the weak scale M_Z . Nevertheless, it can be shown that $I_\alpha \approx 1$ (for $\alpha = e, \mu, \tau$) hold as an excellent approximation in the standard model. This interesting feature implies that the important relations obtained in Eq. (11) hold approximately both at Λ and M_Z . In other words, if a seesaw or flavor symmetry model predicts a hybrid texture of M_ν at Λ , one may simply study its phenomenological consequences at M_Z by taking account of the same texture zero and equality. However, the absolute values of neutrino masses are indeed changed when running from a high-energy scale to low-energy scales.

3 Analytical Approximations

First of all, we point out that there exists a permutation symmetry, which relates one texture to another in Eqs. (1)–(6). More explicitly, the permutation between 2- and 3-rows of M_ν , and that between 2- and 3-columns at the same time, change the position of one zero and two equal elements, giving rise to another hybrid texture \tilde{M}_ν . If M_ν can be diagonalized by a unitary matrix U with mixing parameters $(\theta_{12}, \theta_{23}, \theta_{13}, \delta)$, while \tilde{M}_ν by a unitary matrix \tilde{U} with mixing parameters $(\tilde{\theta}_{12}, \tilde{\theta}_{23}, \tilde{\theta}_{13}, \tilde{\delta})$, it is straightforward to show that these two sets of mixing parameters are related as follows [12]:

$$\tilde{\theta}_{12} = \theta_{12} , \quad \tilde{\theta}_{13} = \theta_{13} , \quad \tilde{\theta}_{23} = \frac{\pi}{2} - \theta_{23} , \quad \tilde{\delta} = \pi - \delta . \quad (20)$$

Moreover, M_ν and \tilde{M}_ν have the same eigenvalues λ_i (for $i = 1, 2, 3$). Among 39 viable patterns, one can immediately verify that such a permutation symmetry exists between

$$\begin{aligned} \mathbf{A}_1 &\leftrightarrow \mathbf{A}_3 , & \mathbf{B}_1 &\leftrightarrow \mathbf{C}_1 , & \mathbf{B}_2 &\leftrightarrow \mathbf{C}_3 , & \mathbf{B}_3 &\leftrightarrow \mathbf{C}_2 , & \mathbf{B}_4 &\leftrightarrow \mathbf{C}_5 , \\ \mathbf{B}_5 &\leftrightarrow \mathbf{C}_4 , & \mathbf{D}_1 &\leftrightarrow \mathbf{D}_2 , & \mathbf{D}_3 &\leftrightarrow \mathbf{D}_6 , & \mathbf{D}_4 &\leftrightarrow \mathbf{D}_5 , & \mathbf{E}_1 &\leftrightarrow \mathbf{F}_2 , \\ \mathbf{E}_2 &\leftrightarrow \mathbf{F}_1 , & \mathbf{E}_3 &\leftrightarrow \mathbf{F}_4 , & \mathbf{E}_4 &\leftrightarrow \mathbf{F}_3 , & \mathbf{E}_5 &\leftrightarrow \mathbf{F}_5 , & \mathbf{E}_6 &\leftrightarrow \mathbf{F}_9 , \\ \mathbf{E}_7 &\leftrightarrow \mathbf{F}_8 , & \mathbf{E}_8 &\leftrightarrow \mathbf{F}_7 , & \mathbf{E}_9 &\leftrightarrow \mathbf{F}_6 , & \mathbf{E}_{10} &\leftrightarrow \mathbf{F}_{10} , \end{aligned} \quad (21)$$

so the analytical results in Eq. (11) for one hybrid texture can be obtained from those for the corresponding paired one. Hence we are left with only twenty independent patterns. It is worthwhile to mention that **Pattern A₂** is invariant under the permutations of 2- and 3-rows and columns.

In the following, we focus on the approximate analytical results for the six patterns **A₁**, **B₁**, **B₅**, **D₁**, **E₁**, and **E₈** and explore their implications for neutrino mass spectrum and the leptonic CP-violating phases. The detailed numerical studies will be given in section 4. The analytical approximations for the other patterns can be discussed in a similar way, but they are more or less dependent on whether the mixing angle θ_{23} is close to $\pi/4$ and whether the Dirac CP-violating phase δ is nearly $\pi/2$. Another important motivation to choose these six patterns for illustration is that they provide very concrete predictions either for the mixing angles, or for the neutrino mass hierarchy, or for the Dirac CP-violating phase, or for the neutrinoless double-beta decays, which make them phenomenologically more interesting and experimentally more testable than the other patterns.

- **Pattern A₁** with $(M_\nu)_{ee} = 0$ and $(M_\nu)_{\mu\mu} = (M_\nu)_{\mu\tau}$. With the help of Eq. (11), in the leading order of $\sin \theta_{13}$, we have

$$\begin{aligned} \frac{\lambda_1}{\lambda_3} &\approx -\frac{\sin^2 \theta_{12} (1 - \tan \theta_{23})}{\cos 2\theta_{12} (1 + \cot \theta_{23})} e^{2i\delta} , \\ \frac{\lambda_2}{\lambda_3} &\approx +\frac{\cos^2 \theta_{12} (1 - \tan \theta_{23})}{\cos 2\theta_{12} (1 + \cot \theta_{23})} e^{2i\delta} , \end{aligned} \quad (22)$$

which lead us to the neutrino mass ratios

$$\begin{aligned}\xi &\approx \frac{\sin^2 \theta_{12} |1 - \tan \theta_{23}|}{\cos 2\theta_{12} (1 + \cot \theta_{23})}, \\ \zeta &\approx \frac{\cos^2 \theta_{12} |1 - \tan \theta_{23}|}{\cos 2\theta_{12} (1 + \cot \theta_{23})},\end{aligned}\quad (23)$$

and the relations between Majorana and Dirac CP-violating phases: $\rho \approx \delta - \pi/2$ and $\sigma \approx \delta$ (for $\theta_{23} < 45^\circ$) or $\rho \approx \delta$ and $\sigma \approx \delta - \pi/2$ (for $\theta_{23} > 45^\circ$).

Taking the 3σ ranges of neutrino mixing angles, we obtain $0.59 \leq \tan \theta_{12} \leq 0.75$ and $0.70 \leq \tan \theta_{23} \leq 1.3$, which yield $\xi < \zeta < 1$. Therefore, only the normal neutrino mass hierarchy $m_1 < m_2 < m_3$ or equivalently $\Delta m^2 > 0$ is allowed. Furthermore, we get

$$R_\nu \approx \zeta^2 - \xi^2 \approx \sec 2\theta_{12} \left(\frac{1 - \tan \theta_{23}}{1 + \cot \theta_{23}} \right)^2, \quad (24)$$

which is actually independent of δ . In order to determine or constrain δ , we have to work in the next-to-leading order approximation. More explicitly, we obtain

$$\begin{aligned}\xi &\approx \frac{\sin^2 \theta_{12} |1 - \tan \theta_{23}|}{\cos 2\theta_{12} (1 + \cot \theta_{23})} \left(1 + \frac{1 - \cot 2\theta_{23}}{1 + \cot \theta_{23}} \tan 2\theta_{12} \sin \theta_{13} \cos \delta \right), \\ \zeta &\approx \frac{\cos^2 \theta_{12} |1 - \tan \theta_{23}|}{\cos 2\theta_{12} (1 + \cot \theta_{23})} \left(1 + \frac{1 - \cot 2\theta_{23}}{1 + \cot \theta_{23}} \tan 2\theta_{12} \sin \theta_{13} \cos \delta \right),\end{aligned}\quad (25)$$

and thus

$$R_\nu \approx \sec 2\theta_{12} \left(\frac{1 - \tan \theta_{23}}{1 + \cot \theta_{23}} \right)^2 \left[1 + 2 \tan 2\theta_{12} \sin \theta_{13} \cos \delta \left(\frac{1 - \cot 2\theta_{23}}{1 + \cot \theta_{23}} \right) \right]. \quad (26)$$

Now it is straightforward to solve Eq. (26) for the CP-violating phase, namely,

$$\delta \approx \cos^{-1} \left\{ \frac{\cot 2\theta_{12} (1 + \cot \theta_{23})}{2 \sin \theta_{13} (1 - \cot 2\theta_{23})} \left[\frac{R_\nu (1 + \cot \theta_{23})^2}{\sec 2\theta_{12} (1 - \tan \theta_{23})^2} - 1 \right] \right\}. \quad (27)$$

For the best-fit values of $(\theta_{12}, \theta_{23}, \theta_{13})$ and R_ν from Table 1, there is no solution to Eq. (27). Taking $\theta_{12} = 35^\circ$ and setting the other parameters to their best-fit values (i.e., $\theta_{23} = 38.4^\circ, \theta_{13} = 8.9^\circ, \delta m^2 = 7.54 \times 10^{-5} \text{ eV}^2$ and $\Delta m^2 = 2.43 \times 10^{-3} \text{ eV}^2$), one can figure out the Dirac and Majorana CP-violating phases

$$\delta \approx 23^\circ, \quad \rho \approx -67^\circ, \quad \sigma \approx 23^\circ, \quad (28)$$

as well as the neutrino mass spectrum

$$\begin{aligned}m_3 &\approx \sqrt{\Delta m^2} \approx 4.9 \times 10^{-2} \text{ eV}, \\ m_2 &\approx m_3 \zeta \approx 8.9 \times 10^{-3} \text{ eV}, \\ m_1 &\approx m_3 \xi \approx 4.3 \times 10^{-3} \text{ eV}.\end{aligned}\quad (29)$$

Since $(M_\nu)_{ee} = 0$ holds for **Pattern A**₁, the effective neutrino mass $\langle m \rangle_{ee}$ in the neutrinoless double-beta ($0\nu 2\beta$) decays is vanishing. The future observation of $0\nu 2\beta$ decays will definitely rule out this pattern. See, e.g., Ref. [29], for recent reviews on the theoretical and experimental status of the $0\nu 2\beta$ decays.

- **Pattern \mathbf{B}_1** with $(M_\nu)_{e\mu} = 0$ and $(M_\nu)_{ee} = (M_\nu)_{e\tau}$. In the leading order of $\sin \theta_{13}$, one can obtain from Eq. (11) that

$$\begin{aligned}\frac{\lambda_1}{\lambda_3} &\approx \frac{\sin \theta_{13}}{\cos \theta_{23}} (1 + \tan \theta_{12} \sin \theta_{23} e^{i\delta}) , \\ \frac{\lambda_2}{\lambda_3} &\approx \frac{\sin \theta_{13}}{\cos \theta_{23}} (1 - \cot \theta_{12} \sin \theta_{23} e^{i\delta}) ,\end{aligned}\quad (30)$$

leading to the neutrino mass ratios

$$\begin{aligned}\xi &\approx \frac{\sin \theta_{13}}{\cos \theta_{23}} (1 + \tan^2 \theta_{12} \sin^2 \theta_{23} + 2 \tan \theta_{12} \sin \theta_{23} \cos \delta)^{1/2} , \\ \zeta &\approx \frac{\sin \theta_{13}}{\cos \theta_{23}} (1 + \cot^2 \theta_{12} \sin^2 \theta_{23} - 2 \cot \theta_{12} \sin \theta_{23} \cos \delta)^{1/2} ,\end{aligned}\quad (31)$$

and the Majorana CP-violating phases

$$\begin{aligned}\rho &\approx \frac{1}{2} \arg (1 + \tan \theta_{12} \sin \theta_{23} e^{i\delta}) , \\ \sigma &\approx \frac{1}{2} \arg (1 - \cot \theta_{12} \sin \theta_{23} e^{i\delta}) .\end{aligned}\quad (32)$$

Taking the values of three neutrino mixing angles $(\theta_{12}, \theta_{23}, \theta_{13})$ within their 3σ ranges, one can verify $\xi < \zeta < 1$, implying that only the normal neutrino mass hierarchy ($m_1 < m_2 < m_3$) is allowed. Furthermore, we obtain

$$R_\nu \approx \zeta^2 - \xi^2 \approx 4 \sin^2 \theta_{13} \csc 2\theta_{12} \tan^2 \theta_{23} (\cot 2\theta_{12} - \csc \theta_{23} \cos \delta), \quad (33)$$

from which one can determine the CP-violating phase

$$\delta \approx \cos^{-1} \left[\sin \theta_{23} \left(\cot 2\theta_{12} - \frac{R_\nu \sin 2\theta_{12}}{4 \sin^2 \theta_{13} \tan^2 \theta_{23}} \right) \right]. \quad (34)$$

Since neutrino oscillation experiments indicate $m_1 < m_2$ (i.e., $R_\nu > 0$), the condition $\cos \delta < \cot 2\theta_{12} \sin \theta_{23}$ should be satisfied. With the best-fit values of three neutrino mixing angles and two neutrino mass-squared differences given in Table 1, we arrive at

$$\delta \approx 92^\circ, \quad \rho \approx 11^\circ, \quad \sigma \approx -21^\circ, \quad (35)$$

while three neutrino masses are

$$\begin{aligned}m_3 &\approx \sqrt{|\Delta m^2|} \approx 4.9 \times 10^{-2} \text{ eV} , \\ m_2 &\approx m_3 \zeta \approx 1.4 \times 10^{-2} \text{ eV} , \\ m_1 &\approx m_3 \xi \approx 1.0 \times 10^{-2} \text{ eV} .\end{aligned}\quad (36)$$

In addition, the effective neutrino mass in the $0\nu 2\beta$ decays can be estimated as $\langle m \rangle_{ee} \approx m_3 \sin \theta_{13} \sec \theta_{23} \approx 9.8 \times 10^{-3} \text{ eV}$, which is quite challenging for the experimental searches even at the next-generation facilities [29].

- **Pattern \mathbf{B}_5** with $(M_\nu)_{e\mu} = 0$ and $(M_\nu)_{\mu\tau} = (M_\nu)_{\tau\tau}$. With the help of Eq. (11), in the leading order of $\sin \theta_{13}$, we get

$$\frac{\lambda_1}{\lambda_3} \approx \frac{\lambda_2}{\lambda_3} \approx \frac{e^{2i\delta} (1 - \cot \theta_{23})}{1 + \tan \theta_{23}}, \quad (37)$$

from which follows

$$\xi \approx \zeta \approx \frac{|1 - \cot \theta_{23}|}{1 + \tan \theta_{23}}, \quad (38)$$

and $\rho \approx \sigma \approx \delta - \pi/2$ (for $\theta_{23} < 45^\circ$) or $\rho \approx \sigma \approx \delta$ (for $\theta_{23} > 45^\circ$). Since $R_\nu \approx 0$ in the leading-order approximation, we have to work at the next-to-leading order

$$\begin{aligned} \frac{\lambda_1}{\lambda_3} &\approx \frac{e^{2i\delta} (1 - \cot \theta_{23})}{1 + \tan \theta_{23}} \left[1 + \frac{\sin \theta_{13} \cos \delta [1 - i\sqrt{2} \tan \delta \sin(2\theta_{23} - \pi/4)]}{\tan \theta_{12} \cos^2 \theta_{23} (1 - \cot \theta_{23})} \right], \\ \frac{\lambda_2}{\lambda_3} &\approx \frac{e^{2i\delta} (1 - \cot \theta_{23})}{1 + \tan \theta_{23}} \left[1 - \frac{\sin \theta_{13} \cos \delta [1 - i\sqrt{2} \tan \delta \sin(2\theta_{23} - \pi/4)]}{\cot \theta_{12} \cos^2 \theta_{23} (1 - \cot \theta_{23})} \right]. \end{aligned} \quad (39)$$

Hence, to the first order of $\sin \theta_{13}$, one obtains

$$R_\nu \approx \zeta^2 - \xi^2 \approx \frac{2(1 - \tan \theta_{23}) \sin \theta_{13} \cos \delta}{(1 - \cot 2\theta_{23}) \sin 2\theta_{12}}, \quad (40)$$

leading to

$$\delta \approx \cos^{-1} \left[\frac{(1 - \cot 2\theta_{23}) \sin 2\theta_{12} R_\nu}{2(1 - \tan \theta_{23}) \sin \theta_{13}} \right], \quad (41)$$

and the difference between two neutrino mass ratios

$$\zeta - \xi \approx \frac{(1 - \tan^2 \theta_{23}) \sin \theta_{13} \cos \delta}{(1 - \cot 2\theta_{23}) |1 - \cot \theta_{23}| \sin 2\theta_{12}}. \quad (42)$$

Taking the values of θ_{23} within the 3σ range, we have $\xi \approx \zeta < 1$, implying that only the normal neutrino mass hierarchy is allowed. To ensure $\xi < \zeta$ or equivalently $m_1 < m_2$, we have to require $\cos \delta > 0$ for $\theta_{23} < 45^\circ$, and $\cos \delta < 0$ for $\theta_{23} > 45^\circ$. Furthermore, using the best-fit values of three neutrino mixing angles and two neutrino mass-squared differences, we arrive at

$$\delta \approx 70^\circ, \quad \rho \approx 12^\circ, \quad \sigma \approx -30^\circ, \quad (43)$$

and the neutrino mass spectrum

$$\begin{aligned} m_3 &\approx (1 + \tan \theta_{23}) \sqrt{\frac{\Delta m^2 \sin 2\theta_{23}}{1 - \cot 2\theta_{23}}} \approx 5.0 \times 10^{-2} \text{ eV}, \\ m_1 &\approx m_2 \approx m_3 \cdot \frac{|1 - \cot \theta_{23}|}{1 + \tan \theta_{23}} \approx 7.3 \times 10^{-3} \text{ eV}. \end{aligned} \quad (44)$$

It is straightforward to calculate the effective neutrino mass $\langle m \rangle_{ee} \approx 7.3 \times 10^{-3} \text{ eV}$ in the $0\nu 2\beta$ decays. As expected for the case of normal neutrino mass hierarchy, $\langle m \rangle_{ee}$ is too small to be measured in the near future.

- **Pattern D₁** with $(M_\nu)_{\mu\tau} = 0$ and $(M_\nu)_{ee} = (M_\nu)_{e\mu}$. From Eq. (11), in the leading order of $\sin\theta_{13}$, we derive

$$\begin{aligned}\frac{\lambda_1}{\lambda_3} &\approx e^{2i\delta} \frac{\cos\theta_{23} - \tan\theta_{12}e^{i\delta}}{\cos\theta_{23} + 2\cot 2\theta_{12}e^{i\delta}}, \\ \frac{\lambda_2}{\lambda_3} &\approx e^{2i\delta} \frac{\cos\theta_{23} + \cot\theta_{12}e^{i\delta}}{\cos\theta_{23} + 2\cot 2\theta_{12}e^{i\delta}}.\end{aligned}\quad (45)$$

From Eq. (45), it is straightforward to extract the neutrino mass ratios

$$\begin{aligned}\xi &\approx \left[\frac{\cos^2\theta_{23} + \tan^2\theta_{12} - 2\cos\delta\cos\theta_{23}\tan\theta_{12}}{\cos^2\theta_{23} + 4\cot^2 2\theta_{12} + 4\cos\delta\cot 2\theta_{12}\cos\theta_{23}} \right]^{1/2}, \\ \zeta &\approx \left[\frac{\cos^2\theta_{23} + \cot^2\theta_{12} + 2\cos\delta\cos\theta_{23}\cot\theta_{12}}{\cos^2\theta_{23} + 4\cot^2 2\theta_{12} + 4\cos\delta\cot 2\theta_{12}\cos\theta_{23}} \right]^{1/2},\end{aligned}\quad (46)$$

and the Majorana CP-violating phases

$$\begin{aligned}\rho &\approx \delta + \frac{1}{2} \arg \left[\frac{\cos\theta_{23} - \tan\theta_{12}e^{i\delta}}{\cos\theta_{23} + 2\cot 2\theta_{12}e^{i\delta}} \right], \\ \sigma &\approx \delta + \frac{1}{2} \arg \left[\frac{\cos\theta_{23} + \cot\theta_{12}e^{i\delta}}{\cos\theta_{23} + 2\cot 2\theta_{12}e^{i\delta}} \right].\end{aligned}\quad (47)$$

Moreover, it is easy to show that $\cos\delta > -\cot 2\theta_{12}\sec\theta_{23}$ must be satisfied in order to guarantee $\zeta > \xi$ or equivalently $m_2 > m_1$. Inputting the neutrino mixing angles in their 3σ ranges and $\delta \in [0, 2\pi)$, we find $\zeta > \xi > 1$, so only the inverted neutrino mass hierarchy is possible. Thus we get

$$R_\nu = \frac{2(\zeta^2 - \xi^2)}{(\zeta^2 + \xi^2) - 2} \approx -\frac{8(\cos 2\theta_{12} + \sin 2\theta_{12}\cos\theta_{23}\cos\delta)}{1 + 3\cos 4\theta_{12} + 2\sin 4\theta_{12}\cos\theta_{23}\cos\delta}, \quad (48)$$

which leads us to

$$\delta \approx \cos^{-1} \left[-\frac{8\cos 2\theta_{12} + (1 + 3\cos 4\theta_{12})R_\nu}{4\cos\theta_{23}\sin 2\theta_{12}(2 + \cos 2\theta_{12}R_\nu)} \right]. \quad (49)$$

With the best-fit values of three neutrino mixing angles and two neutrino mass-squared differences, we obtain three CP-violating phases

$$\delta \approx 122^\circ, \quad \rho \approx 76^\circ, \quad \sigma \approx -45^\circ, \quad (50)$$

and three neutrino masses

$$\begin{aligned}m_3 &\approx \sqrt{\frac{\delta m^2}{\zeta^2 - \xi^2}} \approx 3.91 \times 10^{-2} \text{ eV}, \\ m_2 &\approx m_3\zeta \approx 6.32 \times 10^{-2} \text{ eV}, \\ m_1 &\approx m_3\xi \approx 6.26 \times 10^{-2} \text{ eV}.\end{aligned}\quad (51)$$

Note that the neutrino mass spectrum is nearly degenerate, so the effective neutrino mass in the $0\nu 2\beta$ decays $\langle m \rangle_{ee} \approx m_3/|1 + 2e^{i\delta}\cot 2\theta_{12}\sec\theta_{23}| \approx 3.87 \times 10^{-2} \text{ eV}$ turns out to be accessible in the next-generation experiments.

- **Pattern \mathbf{E}_1** with $(M_\nu)_{\mu\mu} = 0$ and $(M_\nu)_{ee} = (M_\nu)_{e\mu}$. With the help of Eq. (11), in the leading order of $\sin \theta_{13}$, we have

$$\begin{aligned}\frac{\lambda_1}{\lambda_3} &\approx -e^{2i\delta} \tan^2 \theta_{23} \frac{\cos \theta_{23} - \tan \theta_{12} e^{i\delta}}{\cos \theta_{23} + 2 \cot 2\theta_{12} e^{i\delta}}, \\ \frac{\lambda_2}{\lambda_3} &\approx -e^{2i\delta} \tan^2 \theta_{23} \frac{\cos \theta_{23} + \cot \theta_{12} e^{i\delta}}{\cos \theta_{23} + 2 \cot 2\theta_{12} e^{i\delta}}.\end{aligned}\quad (52)$$

From Eq. (52), it is straightforward to extract the neutrino mass ratios

$$\begin{aligned}\xi &\approx \tan^2 \theta_{23} \left[\frac{\cos^2 \theta_{23} + \tan^2 \theta_{12} - 2 \cos \delta \cos \theta_{23} \tan \theta_{12}}{\cos^2 \theta_{23} + 4 \cot^2 2\theta_{12} + 4 \cos \delta \cot 2\theta_{12} \cos \theta_{23}} \right]^{1/2}, \\ \zeta &\approx \tan^2 \theta_{23} \left[\frac{\cos^2 \theta_{23} + \cot^2 \theta_{12} + 2 \cos \delta \cos \theta_{23} \cot \theta_{12}}{\cos^2 \theta_{23} + 4 \cot^2 2\theta_{12} + 4 \cos \delta \cot 2\theta_{12} \cos \theta_{23}} \right]^{1/2},\end{aligned}\quad (53)$$

and the Majorana CP-violating phases

$$\begin{aligned}\rho &\approx \delta + \frac{1}{2} \arg \left[\frac{-\cos \theta_{23} + \tan \theta_{12} e^{i\delta}}{\cos \theta_{23} + 2 \cot 2\theta_{12} e^{i\delta}} \right], \\ \sigma &\approx \delta + \frac{1}{2} \arg \left[\frac{-\cos \theta_{23} - \cot \theta_{12} e^{i\delta}}{\cos \theta_{23} + 2 \cot 2\theta_{12} e^{i\delta}} \right].\end{aligned}\quad (54)$$

Combining Eq. (53) with Eq. (12), we can determine the Dirac CP-violating phase

$$\delta \approx \cos^{-1} \left\{ -\frac{\cot 2\theta_{12}}{\cos \theta_{23}} \left[1 + \frac{\tan^2 2\theta_{12} (\cot^4 \theta_{23} - \csc^2 \theta_{23}) R_\nu}{4 \sec 2\theta_{12} + 2 (2 \cot^4 \theta_{23} - 1) R_\nu} \right] \right\}. \quad (55)$$

Taking the best-fit values of three neutrino mixing angles and two neutrino mass-squared differences, we obtain

$$\delta \approx 122^\circ, \quad \rho \approx -13^\circ, \quad \sigma \approx 45^\circ, \quad (56)$$

and the neutrino mass spectrum is as follows

$$\begin{aligned}m_3 &\approx \sqrt{\frac{\delta m^2}{\zeta^2 - \xi^2}} \approx 9.24 \times 10^{-2} \text{ eV}, \\ m_1 &\approx m_2 \approx 9.41 \times 10^{-2} \text{ eV}.\end{aligned}\quad (57)$$

Finally, it is straightforward to figure out $\langle m \rangle_{ee} \approx m_3 \tan^2 \theta_{23} / |1 + 2e^{i\delta} \cot 2\theta_{12} \sec \theta_{23}| \approx 5.8 \times 10^{-2} \text{ eV}$, which is quite encouraging for the upcoming $0\nu 2\beta$ experiments.

It is worthwhile to mention that the analytical formulas for **Pattern \mathbf{D}_1** are identical to those for **Pattern \mathbf{E}_1** if $\theta_{23} = \pi/4$ is assumed. Therefore, the precision measurement of θ_{23} is crucial to distinguish between these two patterns of M_ν .

- **Pattern \mathbf{E}_8** with $(M_\nu)_{\mu\mu} = 0$ and $(M_\nu)_{e\tau} = (M_\nu)_{\mu\tau}$. From Eq. (11), in the leading order of $\sin \theta_{13}$, we obtain

$$\begin{aligned}\frac{\lambda_1}{\lambda_3} &\approx -e^{2i\delta} (\tan^2 \theta_{23} - \cot \theta_{12} \sec \theta_{23} e^{-i\delta}), \\ \frac{\lambda_2}{\lambda_3} &\approx -e^{2i\delta} (\tan^2 \theta_{23} + \tan \theta_{12} \sec \theta_{23} e^{-i\delta}).\end{aligned}\quad (58)$$

Then, from Eq. (58), it is easy to extract the neutrino mass ratios

$$\begin{aligned}\xi &\approx [\tan^4 \theta_{23} + \cot^2 \theta_{12} \sec^2 \theta_{23} - 2 \cot \theta_{12} \tan^2 \theta_{23} \sec \theta_{23} \cos \delta]^{1/2}, \\ \zeta &\approx [\tan^4 \theta_{23} + \tan^2 \theta_{12} \sec^2 \theta_{23} + 2 \tan \theta_{12} \tan^2 \theta_{23} \sec \theta_{23} \cos \delta]^{1/2},\end{aligned}\quad (59)$$

and the Majorana CP-violating phases

$$\begin{aligned}\rho &\approx \delta + \frac{1}{2} \arg [-\tan^2 \theta_{23} + \cot \theta_{12} \sec \theta_{23} e^{-i\delta}], \\ \sigma &\approx \delta + \frac{1}{2} \arg [-\tan^2 \theta_{23} - \tan \theta_{12} \sec \theta_{23} e^{-i\delta}].\end{aligned}\quad (60)$$

One immediately observes from Eq. (59) that

$$\zeta^2 - \xi^2 \approx \frac{4(\cos \delta \tan^2 \theta_{23} - \cot 2\theta_{12} \sec \theta_{23})}{\sin 2\theta_{12} \cos \theta_{23}}. \quad (61)$$

In order to ensure $m_1 < m_2$ or equivalently $\zeta^2 - \xi^2 > 0$, we have to require $\cos \delta > \cot 2\theta_{12} \sec \theta_{23} \cot^2 \theta_{23} > 0$, implying $\delta < \pi/2$ or $\delta > 3\pi/2$. Taking the 3σ ranges of the mixing parameters, we find that only the inverted neutrino mass hierarchy is allowed. Moreover, we get

$$R_\nu \approx \frac{4 \csc 2\theta_{12} (\cos \delta \tan^2 \theta_{23} - \cot 2\theta_{12} \sec \theta_{23})}{(2 \cot^2 2\theta_{12} + \tan^2 \theta_{23}) \sec \theta_{23} - 2 \cos \delta \cot 2\theta_{12} \tan^2 \theta_{23}}, \quad (62)$$

from which one can determine the Dirac CP-violating phase

$$\delta \approx \cos^{-1} \left[\frac{\cot 2\theta_{12}}{\tan \theta_{23} \sin \theta_{23}} + \frac{\sin 2\theta_{12} \sec \theta_{23} R_\nu}{4 + 2 \cos 2\theta_{12} R_\nu} \right]. \quad (63)$$

With the best-fit values of three neutrino mixing angles and two neutrino mass-squared differences, we arrive at

$$\delta \approx 30^\circ, \quad \rho \approx 9^\circ, \quad \sigma \approx -68^\circ. \quad (64)$$

In addition, three neutrino masses are found to be

$$\begin{aligned}m_3 &\approx \left[\frac{\delta m^2 \sin 2\theta_{12} \cos \theta_{23}}{4(\cos \delta \tan^2 \theta_{23} - \cot 2\theta_{12} \sec \theta_{23})} \right]^{1/2} \approx 3.61 \times 10^{-2} \text{ eV}, \\ m_2 &\approx m_3 \zeta \approx 5.15 \times 10^{-2} \text{ eV}, \\ m_1 &\approx m_3 \xi \approx 5.11 \times 10^{-2} \text{ eV},\end{aligned}\quad (65)$$

which are nearly degenerate. As a consequence, the effective neutrino mass in the $0\nu 2\beta$ decays $\langle m \rangle_{\text{ee}} \approx m_3 |\tan^2 \theta_{23} e^{i\delta} - 2 \cot 2\theta_{12} \sec \theta_{23}| \approx 2.2 \times 10^{-2} \text{ eV}$ could be probed in the future $0\nu 2\beta$ decay experiments.

The above analytical analyses serve as an explicit example for how to determine the leptonic CP-violating phases and neutrino masses, when a hybrid texture of M_ν is taken. The full parameter space of these patterns will be analyzed in the following section.

4 Numerical Results

As mentioned before, we have performed a numerical study of all the sixty hybrid textures of M_ν . It turns out that thirty-nine of them are consistent with current neutrino oscillation data at the 3σ level, while only thirteen patterns can survive if the 1σ ranges of neutrino mixing parameters are considered. Our numerical analysis has been done in the following way:

- 1) For each pattern of M_ν , we generate a set of random numbers for two neutrino mass-squared differences $(\delta m^2, \Delta m^2)$ and three neutrino mixing angles $(\theta_{12}, \theta_{23}, \theta_{13})$ in their 3σ ranges [23], which have been shown in Table 1. As we have shown in the previous section, it is then possible to determine the Dirac CP-violating phase δ from Eq. (12). Instead, we generate a random number of δ in the range of $[0, 2\pi)$, and test whether Eq. (12) is satisfied by the generated random numbers.
- 2) In practice, with the random numbers above, we first calculate the neutrino mass ratios ζ and ξ , and then three neutrino masses (m_1, m_2, m_3) . The criteria for whether a specific pattern of M_ν is consistent with current experimental data are set as follows: (a) With ζ and ξ , we can determine from Eq. (12) the value of R_ν , which is required to fall into the range $[(\delta m^2)_{\min}^{3\sigma}/(\Delta m^2)_{\max}^{3\sigma}, (\delta m^2)_{\max}^{3\sigma}/(\Delta m^2)_{\min}^{3\sigma}]$. (b) Since only two possible neutrino mass hierarchies $m_1 < m_2 < m_3$ and $m_3 < m_1 < m_2$ are allowed by neutrino oscillation experiments, we further demand $(\xi^2 - 1)(\zeta^2 - 1) > 0$, namely, $\xi^2 < \zeta^2 < 1$ corresponds to the normal mass hierarchy while $\zeta^2 > \xi^2 > 1$ to the inverted mass hierarchy. (c) The absolute scale of neutrino masses receives constraints from the beta-decay and $0\nu 2\beta$ -decay experiments, however, the most restrictive one comes from cosmological observations [30]. Recently, the Planck Collaboration has released the first data on cosmic microwave background (CMB) [31]. Combined with the WMAP-polarization, high-resolution CMB, and BAO data sets, the Planck data have placed an upper bound on the sum of three neutrino masses $\sum m_i < 0.23$ eV at the 95% confidence level. We require that this upper bound should be satisfied. Once one pattern of M_ν survives all the above constraints, we will calculate its predictions for the effective neutrino mass $\langle m \rangle_{ee}$ in the $0\nu 2\beta$ decays, the two Majorana CP-violating phases (ρ, σ) and the Jarlskog invariant for leptonic CP violation $J_{\text{CP}} = s_{12}c_{12}s_{23}c_{23}s_{13}c_{13}^2 \sin \delta$ [32]. In addition, the allowed parameter space of other mixing parameters can be determined.
- 3) To illustrate our results, we present a series of figures for each viable pattern in Figs. 1–6, where each figure consists of twelve plots in four rows. The first row shows the allowed ranges of three flavor mixing angles θ_{12} , θ_{23} and θ_{13} , versus the Dirac CP-violating phase δ . In the second row, the histograms of three mixing angles are given, indicating their distributions in the allowed parameter space. As the ongoing and forthcoming neutrino oscillation experiments will provide us with more precise measurements of three neutrino mixing angles and the Dirac CP-violating phase, our numerical illustrations make it easy to see whether a currently viable hybrid texture can be ruled out by future experimental

data. In the third row, we present the allowed ranges of three neutrino mass eigenvalues (m_1, m_2, m_3) and the effective neutrino mass $\langle m \rangle_{ee}$ versus δ . From these plots, one can immediately figure out which neutrino mass hierarchy is predicted, and whether the effective neutrino mass $\langle m \rangle_{ee}$ is accessible in future $0\nu 2\beta$ experiments. Finally, the Majorana CP-violating phases ρ , σ and the Jarlskog invariant J_{CP} are depicted in the last row. The next-generation long-baseline neutrino oscillation experiments are promising to discover the leptonic CP violation if the Jarlskog invariant J_{CP} is at the percent level [33].

We have carried out a thorough numerical study of all the sixty patterns of M_ν , however, it will render our paper unreadable if all the figures of the viable thirty-nine patterns are presented. Therefore, we will focus only on the six patterns **A**₁, **B**₁, **B**₅, **D**₁, **E**₁, and **E**₈, for which the analytical results have been given in the previous section. Some comments and discussions on the numerical results in Figs. 1–6 are in order.

- **Pattern A₁** – As shown in first row of Fig. 1, the Dirac CP-violating phase δ is essentially unconstrained and the whole range $[0, 2\pi)$ of δ is experimentally allowed. This can be easily understood from Eq. (24), where R_ν is found to be independent of δ and θ_{13} at the leading order. In contrast with the mixing angles θ_{12} and θ_{13} , which are only mildly constrained, the allowed range of θ_{23} splits into two distinct branches: one for $\theta_{23} < 45^\circ$, and the other for $\theta_{23} > 45^\circ$. Moreover, the histogram of θ_{23} in the second row indicates that $\theta_{23} < 45^\circ$ is preferred, in particular the values as small as $\theta_{23} = 35.1^\circ$ at the lower border of the 3σ range. Consequently, the precision measurement of θ_{23} can finally tell us whether this pattern is allowed or not. It is also interesting that the histogram of θ_{13} peaks around $\theta_{13} = 8^\circ$, quite close to the best-fit value. Three neutrino masses are given in the third row, where one can observe that only the normal mass hierarchy (i.e., $m_1 < m_2 < m_3$) is possible. For **Pattern A₁**, the effective neutrino mass in $0\nu 2\beta$ decays is exactly zero, implying some cancellation takes place among the contributions of three neutrino mass eigenstates. In the fourth row, we can see that an approximately linear correlation exists between the Majorana CP phases (ρ, σ) and δ . For a maximal CP-violating phases $\delta = \pi/2$ or $3\pi/2$, the Jarlskog invariant $|J_{CP}| \sim 3\%$ can be achieved.
- **Pattern B₁** – We can see clearly from the first row of Fig. 2 that only two narrow ranges around $\delta = \pi/2$ and $\delta = 3\pi/2$ are experimentally allowed. Although three neutrino mixing angles θ_{12} , θ_{23} and θ_{13} turn out to be arbitrary in their 3σ ranges, the distributions of θ_{23} and θ_{13} seem to peak around their best-fit values (i.e., $\theta_{23} = 38.4^\circ$ and $\theta_{13} = 8.9^\circ$), as shown in the second row. Similar to **Pattern A₁**, only the normal neutrino mass hierarchy (i.e., $m_1 < m_2 < m_3$) is possible, so the effective neutrino mass $\langle m \rangle_{ee}$ is in general small, which renders it very challenging to observe the $0\nu 2\beta$ decays. Since the constraint on δ is quite restrictive, only a small fraction of the parameter space of ρ and σ is allowed. Interestingly, the Jarlskog invariant J_{CP} is predicted to be close to its maximum, i.e., $|J_{CP}| \geq 3\%$, which should be accessible to the next-generation long-baseline neutrino oscillation experiments [33].

- **Pattern B₅** – From the first row of Fig. 3, one can observe that the allowed ranges of δ contain two disjointed regions: one around $\delta = \pi$, and the other around $\delta = 0$ or 2π . This feature becomes clear, if we recall the analytical discussions on **Pattern B₅** in the previous section, where $\cos \delta > 0$ (i.e., $\delta < \pi/2$ or $\delta > 3\pi/2$) for $\theta_{23} < 45^\circ$, and $\cos \delta < 0$ (i.e., $\pi/2 < \delta < 3\pi/2$) for $\theta_{23} > 45^\circ$, are required to guarantee $m_2 > m_1$. While both θ_{12} and θ_{13} are mildly constrained, θ_{23} is restricted to smaller regions far from the maximal mixing. Moreover, there is a strong correlation between θ_{23} and δ . For instance, if $\delta \approx \pi$ is taken, then $\theta_{23} \approx 51^\circ$ holds; if $\delta \approx 0$ or 2π is assumed, then we obtain $\theta_{23} \approx 39^\circ$. As shown in the second row, the distribution of θ_{23} peaks around its best-fit value, namely, $\theta_{23} = 38.4^\circ$. The numerical results in the third row indicate that only the normal mass hierarchy ($m_1 < m_2 < m_3$) is allowed, and the effective neutrino mass $\langle m \rangle_{ee}$ is quite small. The Majorana CP-violating phases (ρ, σ) and the Jarlskog invariant J_{CP} are shown in the last row, where one can observe that the parameter space is tightly constrained.
- **Pattern D₁** – The Dirac CP-violating phase δ falls into $(\pi/2, 3\pi/2)$, as shown in the first row of Fig. 4. It is evident from Eq. (49) that only $\cos \delta < 0$ (i.e., $\pi/2 < \delta < 3\pi/2$) is possible, given the 3σ ranges of mixing parameters. Although the 3σ ranges of three mixing angles are still allowed, only smaller (larger) values of θ_{12} (θ_{23}) can survive if $\delta \approx \pi$ is assumed. In the second row, the distributions of three mixing angles do not show significant preference in any specific ranges. Different from the previous patterns of M_ν , **Pattern D₁** predicts the inverted neutrino mass hierarchy ($m_3 < m_1 < m_2$), as indicated in the third row. Consequently, the effective neutrino mass $\langle m \rangle_{ee}$ is larger than 0.02 eV, which is reachable in next-generation $0\nu 2\beta$ decay experiments. While ρ is restricted to a relatively small range around $\pi/2$ or $-\pi/2$, σ can take any values in $[-\pi/4, \pi/4]$. In addition, the magnitude of Jarlskog invariant J_{CP} could be at the percent level if δ is close to $\pi/2$ or $3\pi/2$.
- **Pattern E₁** – As shown in the first row of Fig. 5, the Dirac CP-violating phase δ is limited to two small regions around $3\pi/4$ and $5\pi/4$. From the second row, we can observe that θ_{12} and θ_{13} show no significant preference in their 3σ ranges, while θ_{23} has two peaks around 37° and 51° . Note that the former peak dominates over the latter and is quite close to the best-fit value of θ_{23} . The neutrino mass spectrum is nearly degenerate, namely, $m_1 \approx m_2 \approx m_3 \approx 0.1$ eV, as shown in the third row. Therefore, the effective neutrino mass $\langle m \rangle_{ee}$ can be as large as 0.05 eV, which is much larger than those in all the previous patterns. In addition, the parameter space of two Majorana CP-violating phases (ρ, σ) and the Jarlskog invariant J_{CP} is strongly constrained. Since $\sin \delta$ is nonzero, the leptonic CP violation is expected.
- **Pattern E₈** – From the first row of Fig. 6, one can see that the Dirac CP-violating phase δ is restricted to the ranges of $\delta < \pi/2$ and $\delta > 3\pi/2$, which are consistent with our analytical results in section 3. The distribution of θ_{23} peaks around 37° , while those of

θ_{12} and θ_{13} do not show significant preference, as shown in the second row. Only the inverted neutrino mass hierarchy ($m_3 < m_1 < m_2$) is allowed, and the effective neutrino mass $\langle m \rangle_{ee}$ turns out to be in the range $[0.025 \text{ eV}, 0.040 \text{ eV}]$, which is accessible in future $0\nu 2\beta$ decay experiments. In the last row, the two Majorana CP-violating phases ρ and σ are found to be linearly correlated with the Dirac CP phase δ .

It is worthwhile to stress that the precision measurements of three neutrino mixing angles, in particular the octant of θ_{23} , as well as the discovery of leptonic CP violation and the $0\nu 2\beta$ decays, are crucially important to distinguish between different hybrid textures of Majorana neutrino mass matrix. For instance, we have also checked that only thirteen hybrid textures (i.e., \mathbf{A}_3 , $\mathbf{C}_{2,5}$, $\mathbf{D}_{1,5,6}$, $\mathbf{E}_{1,4,6,7}$, and $\mathbf{F}_{1,7,8}$) are viable, if the 1σ ranges of neutrino mixing parameters and the Dirac CP-violating phase are taken into account [23]. In addition, the cosmological bound on absolute neutrino masses becomes very relevant. If the upper limit $\sum m_i < 0.44 \text{ eV}$ from the nine-year WMAP observations [30] is used instead of the latest Planck result, two extra patterns

$$\mathbf{B}_6 : \begin{pmatrix} \Delta & 0 & \times \\ 0 & \times & \Delta \\ \times & \Delta & \times \end{pmatrix}, \quad \mathbf{C}_6 : \begin{pmatrix} \Delta & \times & 0 \\ \times & \times & \Delta \\ 0 & \Delta & \times \end{pmatrix}, \quad (66)$$

can survive the oscillation data at the 3σ level.

5 Flavor Symmetry

It has been proved that the texture zeros in the Majorana neutrino mass matrix M_ν can be realized by implementing the Z_n flavor symmetry [20, 21]. Taking the two-zero textures for example, one can demonstrate that the seven viable patterns can be derived from Z_n symmetries in the type-II seesaw model [12]. To illustrate how to realize the hybrid textures of M_ν , we will work in the type-II seesaw model, which extends the scalar sector of the standard model with one or more $SU(2)_L$ scalar triplets [6]. For N scalar triplets, the gauge-invariant Lagrangian relevant for neutrino masses reads

$$-\mathcal{L}_\Delta = \frac{1}{2} \sum_j \sum_{\alpha, \beta} \left(Y_{\Delta_j} \right)_{\alpha\beta} \overline{\ell_{\alpha L}} \Delta_j i \sigma_2 \ell_{\beta L}^c + \text{h.c.}, \quad (67)$$

where α and β run over e, μ and τ , Δ_j denotes the j -th triplet scalar field (for $j = 1, 2, \dots, N$), and Y_{Δ_j} is the corresponding Yukawa coupling matrix. After the triplet scalar acquires its vacuum expectation value $\langle \Delta_j \rangle \equiv v_j$, the Majorana neutrino mass matrix is given by

$$M_\nu = \sum_j Y_{\Delta_j} v_j, \quad (68)$$

where the smallness of v_j is attributed to the largeness of the triplet scalar mass scale [6].

It is worth mentioning that an equality between two matrix elements cannot be achieved by imposing any Abelian symmetries on the Lagrangian in Eq. (67), since the Abelian symmetry group has only one-dimensional irreducible representations and the Yukawa couplings for different representations are not necessarily the same. In this work, we just take the pattern \mathbf{A}_2 as a typical example, i.e.,

$$M_\nu^{\mathbf{A}_2} = \begin{pmatrix} 0 & a & b \\ a & d & c \\ b & c & d \end{pmatrix}. \quad (69)$$

In order to ensure $(M_\nu)_{ee} = 0$, we have to implement a Z_3 symmetry. Furthermore, to guarantee $(M_\nu)_{\mu\mu} = (M_\nu)_{\tau\tau}$, we can make use of an S_3 symmetry, which is the simplest discrete non-Abelian group. In the framework of type-II seesaw model, we find that at least five scalar triplets Δ_i (for $i = 1, 2, 3, 4, 5$) are necessary. The assignments of the scalar triplets and lepton doublets under the Z_3 symmetry are given as follows:

$$\ell_{eL} \sim \omega, \quad \ell_{\mu L}, \ell_{\tau L} \sim \omega^2, \quad \Delta_1, \Delta_2 \sim 1, \quad \Delta_3, \Delta_4, \Delta_5 \sim \omega; \quad (70)$$

while the assignments under the S_3 symmetry are

$$\ell_{eL} \sim \mathbf{1}, \quad \begin{pmatrix} \ell_{\mu L} \\ \ell_{\tau L} \end{pmatrix} \sim \mathbf{2}, \quad \begin{pmatrix} \Delta_1 \\ \Delta_2 \end{pmatrix} \sim \mathbf{2}, \quad \begin{pmatrix} \Delta_3 \\ \Delta_4 \end{pmatrix} \sim \mathbf{2}, \quad \Delta_5 \sim \mathbf{1}. \quad (71)$$

Hence the $S_3 \otimes Z_3$ -invariant Lagrangian relevant for neutrino masses reads

$$\begin{aligned} \mathcal{L}_\nu = & -\frac{1}{2}y_1\overline{\ell_{eL}}(\Delta_1\ell_{\mu L}^c + \Delta_2\ell_{\tau L}^c) - \frac{1}{2}y_2(\overline{\ell_{\mu L}}\Delta_5\ell_{\mu L}^c + \overline{\ell_{\tau L}}\Delta_5\ell_{\tau L}^c) \\ & -\frac{1}{2}y_3[(\overline{\ell_{\mu L}}\Delta_3\ell_{\tau L}^c + \overline{\ell_{\tau L}}\Delta_3\ell_{\mu L}^c) + (\overline{\ell_{\mu L}}\Delta_4\ell_{\mu L}^c - \overline{\ell_{\tau L}}\Delta_4\ell_{\tau L}^c)] + \text{h.c.}, \end{aligned} \quad (72)$$

where we have used the tensor product $\mathbf{2} \otimes \mathbf{2} = \mathbf{1} + \mathbf{1}' + \mathbf{2}$ for the S_3 symmetry group [34]. After the triplet scalar acquires its vacuum expectation value $\langle \Delta_i \rangle = v_i$, the Majorana neutrino mass matrix is given by

$$M_\nu = \begin{pmatrix} 0 & y_1 v_1 & y_1 v_2 \\ y_1 v_1 & y_2 v_5 + y_3 v_4 & 2y_3 v_3 \\ y_1 v_2 & 2y_3 v_3 & y_2 v_5 - y_3 v_4 \end{pmatrix}. \quad (73)$$

Once $v_4 = 0$ is obtained by minimizing the scalar potential, we arrive at the pattern \mathbf{A}_2 in Eq. (69), with $a = y_1 v_1$, $b = y_1 v_2$, $c = 2y_3 v_3$, and $d = y_2 v_5$. On the other hand, we have to ensure that the charged-lepton mass matrix M_l is diagonal. This can be achieved if one introduces two $SU(2)_L$ scalar doublets Φ_1 and Φ_2 , in addition to the standard-model Higgs doublet H , which is a singlet under the flavor symmetry. These two extra scalar doublets and three right-handed charged-lepton fields are assigned as:

$$e_R \sim \omega, \quad \mu_R, \tau_R \sim \omega^2, \quad \Phi_1, \Phi_2 \sim 1 \quad (74)$$

under the Z_3 symmetry, while

$$e_R, \tau_R \sim \mathbf{1}, \quad \mu_R \sim \mathbf{1}', \quad \begin{pmatrix} \Phi_1 \\ \Phi_2 \end{pmatrix} \sim \mathbf{2} \quad (75)$$

under the S_3 symmetry. Three lepton doublets transform in the same way as in Eqs. (70) and (71). Therefore, the $S_3 \otimes Z_3$ -invariant Lagrangian relevant for the charged-lepton masses is

$$\mathcal{L}_l = -y_e \overline{\ell_{eL}} H e_R - y_\mu (\overline{\ell_{\mu L}} \Phi_2 - \overline{\ell_{\tau L}} \Phi_1) \mu_R - y_\tau (\overline{\ell_{\mu L}} \Phi_1 + \overline{\ell_{\tau L}} \Phi_2) \tau_R + \text{h.c.}, \quad (76)$$

leading to a diagonal charged-lepton mass matrix $M_l \equiv \text{Diag}\{m_e, m_\mu, m_\tau\}$ with three mass eigenvalues $m_e = y_e v / \sqrt{2}$, $m_\mu = y_\mu u / \sqrt{2}$, and $m_\tau = y_\tau u / \sqrt{2}$, where the vacuum expectation values of three scalar doublets $\langle H \rangle = v / \sqrt{2}$, $\langle \Phi_2 \rangle = u / \sqrt{2}$ and $\langle \Phi_1 \rangle = 0$ have been taken. Our numerical analysis has demonstrated that the hybrid texture in Eq. (69) is consistent with current neutrino oscillation data at the 3σ level.

To complete the above $S_3 \otimes Z_3$ flavor model, we have to examine in detail the invariant scalar potential and check whether vacuum alignments $v_1 \neq v_2$, $v_3 \neq v_4$, and $\langle \Phi_1 \rangle \neq \langle \Phi_2 \rangle$ can be actually realized. For this purpose, one can work in the supersymmetric version of type-II seesaw model and follow the method of driving flavon fields, as proposed in Refs. [35, 36]. In addition, the symmetry realization of all the thirty-nine viable hybrid textures of M_ν in a systematic way deserves further studies and will be discussed elsewhere.

6 Summary

Motivated by the recent measurements of θ_{13} in reactor neutrino experiments, we have performed a thorough study of the so-called hybrid textures of Majorana neutrino mass matrix M_ν , where one texture zero and one equality between two nonzero matrix elements are assumed. We have found that thirty-nine out of sixty possible patterns are compatible with current experimental data at the 3σ level. In the following, our main results are summarized:

- If three neutrino mixing angles ($\theta_{12}, \theta_{23}, \theta_{13}$) and two neutrino mass-squared differences ($\delta m^2, \Delta m^2$) are given, the leptonic CP-violating phases (ρ, σ, δ) and three neutrino masses (m_1, m_2, m_3) can be fully determined. For illustration, we have chosen six hybrid textures $\mathbf{A}_1, \mathbf{B}_1, \mathbf{B}_5, \mathbf{D}_1, \mathbf{E}_1$, and \mathbf{E}_8 , and derived the analytical approximate formulas for the CP-violating phases and neutrino masses.
- In Figs. 1–6, we show the numerical results for the above six hybrid textures. Some interesting observations should be mentioned: (1) The allowed regions of θ_{23} from the patterns \mathbf{A}_1 and \mathbf{B}_5 turn out to be well separated and deviate significantly from the maximal mixing. Therefore, if θ_{23} is finally measured to be very close to $\pi/4$, then both \mathbf{A}_1 and \mathbf{B}_5 can be excluded. (2) Except the pattern \mathbf{A}_1 , all the hybrid textures under consideration have specific predictions for the CP-violating phase δ . In addition, their

predictions for the effective neutrino mass $\langle m \rangle_{ee}$ could also be quite different. (3) Now the cosmological bound on the absolute scale of neutrino masses becomes quite relevant for the study of lepton flavor structure.

Moreover, we have considered the stability of texture zeros and equality against one-loop quantum corrections. In a type-II seesaw model, we illustrate how to realize the hybrid texture \mathbf{A}_2 by implementing an $S_3 \otimes Z_3$ flavor symmetry.

The ongoing and upcoming neutrino oscillation experiments are expected to precisely measure the neutrino mixing parameters, in particular the smallest mixing angle θ_{13} , the deviation of θ_{23} from $\pi/4$ and the Dirac CP-violating phase δ . The sensitivity of future cosmological observations to the sum of neutrino masses $\sum m_i$ and the sensitivity of the neutrinoless double-beta decay experiments to the effective mass term $\langle m \rangle_{ee}$ will probably reach ~ 0.05 eV in the near future. We therefore expect that many patterns of the hybrid textures of M_ν can be excluded or only marginally allowed by tomorrow's data, and those capable of surviving should shed light on the underlying flavor structures of massive neutrinos.

Acknowledgements

One of the authors (J.Y.L.) would like to thank Prof. Zhi-zhong Xing for inspiring discussions, and Theoretical Physics Division of IHEP for financial support and hospitality during his visit in Beijing, where part of this work was done. This work was supported in part by the National Natural Science Foundation of China under grant No. 11205113 (J.Y.L.) and by the Göran Gustafsson Foundation (S.Z.).

References

- [1] See, e.g., Z.Z. Xing and S. Zhou, *Neutrinos in Particle Physics, Astronomy and Cosmology* (Zhejiang University Press and Springer Verlag, 2011).
- [2] Particle Data Group, J. Beringer *et al.*, Phys. Rev. D **86**, 010001 (2012).
- [3] F.P. An *et al.* (Daya Bay Collaboration), Phys. Rev. Lett. **108**, 171803 (2012); Chin. Phys. C **37**, 011001 (2013).
- [4] J.K. Ahn *et al.* (RENO Collaboration), Phys. Rev. Lett. **108**, 191802 (2012).
- [5] H. Fritzsch, M. Gell-Mann, and P. Minkowski, Phys. Lett. B **59**, 256 (1975); P. Minkowski, Phys. Lett. B **67**, 421 (1977); T. Yanagida, in *Proceedings of the Workshop on Unified Theory and the Baryon Number of the Universe*, edited by O. Sawada and A. Sugamoto (KEK, Tsukuba, 1979), p. 95; M. Gell-Mann, P. Ramond, and R. Slansky, in *Supergravity*, edited by P. van Nieuwenhuizen and D.Z. Freeman (North-Holland, Amsterdam, 1979), p. 315; S.L. Glashow, in *Quarks and Leptons*, edited by M. Levy *et al.* (Plenum, New York, 1980), p. 707; R.N. Mohapatra and G. Senjanovic, Phys. Rev. Lett. **44**, 912 (1980).
- [6] W. Konetschny and W. Kummer, Phys. Lett. B **70**, 433 (1977); J. Schechter and J.W.F. Valle, Phys. Rev. D **22**, 2227 (1980); T.P. Cheng and L.F. Li, Phys. Rev. D **22**, 2860 (1980); M. Magg and C. Wetterich, Phys. Lett. B **94**, 61 (1980); G. Lazarides, Q. Shafi, and C. Wetterich, Nucl. Phys. B **181**, 287 (1981); R.N. Mohapatra and G. Senjanovic, Phys. Rev. D **23**, 165 (1981).
- [7] R. Foot, H. Lew, X.G. He, and G.C. Joshi, Z. Phys. C **44**, 441 (1989).
- [8] P.H. Frampton, S.L. Glashow, and D. Marfatia, Phys. Lett. B **536**, 79 (2002).
- [9] Z.Z. Xing, Phys. Lett. B **530**, 159 (2002).
- [10] Z.Z. Xing, Phys. Lett. B **539**, 85 (2002).
- [11] W.L. Guo and Z.Z. Xing, Phys. Rev. D **67**, 053002 (2003).
- [12] H. Fritzsch, Z.Z. Xing, and S. Zhou, JHEP **1109**, 083 (2011).
- [13] P.O. Ludl, S. Morisi, and E. Peinado, Nucl. Phys. B **857**, 411 (2012); D. Meloni and G. Blankenburg, Nucl. Phys. B **867**, 749 (2013).
- [14] W. Grimus and P.O. Ludl, JHEP **1212**, 117 (2012); J. Phys. G **40**, 055003 (2013).
- [15] S. Kaneko, H. Sawanaka, and M. Tanimoto, JHEP **0508**, 073 (2005).
- [16] S. Dev, S. Verma, and S. Gupta, Phys. Lett. B **687**, 53 (2010).

- [17] S. Goswami, S. Khan, and A. Watanabe, Phys. Lett. B **693**, 249 (2010); A. Dighe and N. Sahu, arXiv:0812.0695 [hep-ph];
- [18] S. Dev, R.R. Gautam, and L. Singh, Phys. Rev. D **87**, 073011 (2013).
- [19] M. Frigerio and A.V. del Moral, arXiv:1303.5284 [hep-ph].
- [20] W. Grimus, A.S. Joshipura, L. Lavoura, and M. Tanimoto, Eur. Phys. J. C **36**, 227 (2004).
- [21] W. Grimus and L. Lavoura, J. Phys. G **31**, 693 (2005); Z.Z. Xing and S. Zhou, Phys. Lett. B **679**, 249 (2009).
- [22] T. Araki, J. Heeck, and J. Kubo, JHEP **1207**, 083 (2012).
- [23] G.L. Fogli, E. Lisi, A. Marrone, D. Montanino, A. Palazzo, and A.M. Rotunno, Phys. Rev. D **86**, 013012 (2012).
- [24] M.C. Gonzalez-Garcia, M. Maltoni, J. Salvado, and T. Schwetz, JHEP **1212**, 123 (2012).
- [25] D.V. Forero, M. Tórtola, and J.W.F. Valle, Phys. Rev. D **86**, 073012 (2012).
- [26] S. Weinberg, Phys. Rev. Lett. **43**, 1566 (1979).
- [27] See, e.g., P.H. Chankowski and Z. Pluciennik, Phys. Lett. B **316**, 312 (1993); K.S. Babu, C.N. Leung, and J. Pantaleone, Phys. Lett. B **319**, 191 (1993).
- [28] J.W. Mei and Z.Z. Xing, Phys. Rev. D **69**, 073003 (2004).
- [29] W. Rodejohann, Int. J. Mod. Phys. E **20**, 1833 (2011); J. Phys. G **39**, 124008 (2012).
- [30] G. Hinshaw *et al.* (WMAP Collaboration), arXiv:1212.5226 [astro-ph.CO].
- [31] P.A.R. Ade *et al.* (Planck Collaboration), arXiv:1303.5076 [astro-ph.CO].
- [32] C. Jarlskog, Phys. Rev. Lett. **55**, 1039 (1985); D.D. Wu, Phys. Rev. D **33**, 860 (1986).
- [33] G.C. Branco, R.G. Felipe, and F.R. Joaquim, Rev. Mod. Phys. **84**, 515 (2012).
- [34] H. Ishimori, T. Kobayashi, H. Ohki, Y. Shimizu, H. Okada, and M. Tanimoto, Prog. Theor. Phys. Suppl. **183**, 1 (2010).
- [35] G. Altarelli and F. Feruglio, Nucl. Phys. B **720**, 64 (2005); Nucl. Phys. B **741**, 215 (2006).
- [36] G. Altarelli and F. Feruglio, Rev. Mod. Phys. **82**, 2701 (2010); S.F. King and C. Luhn, Rept. Prog. Phys. **76**, 056201 (2013).

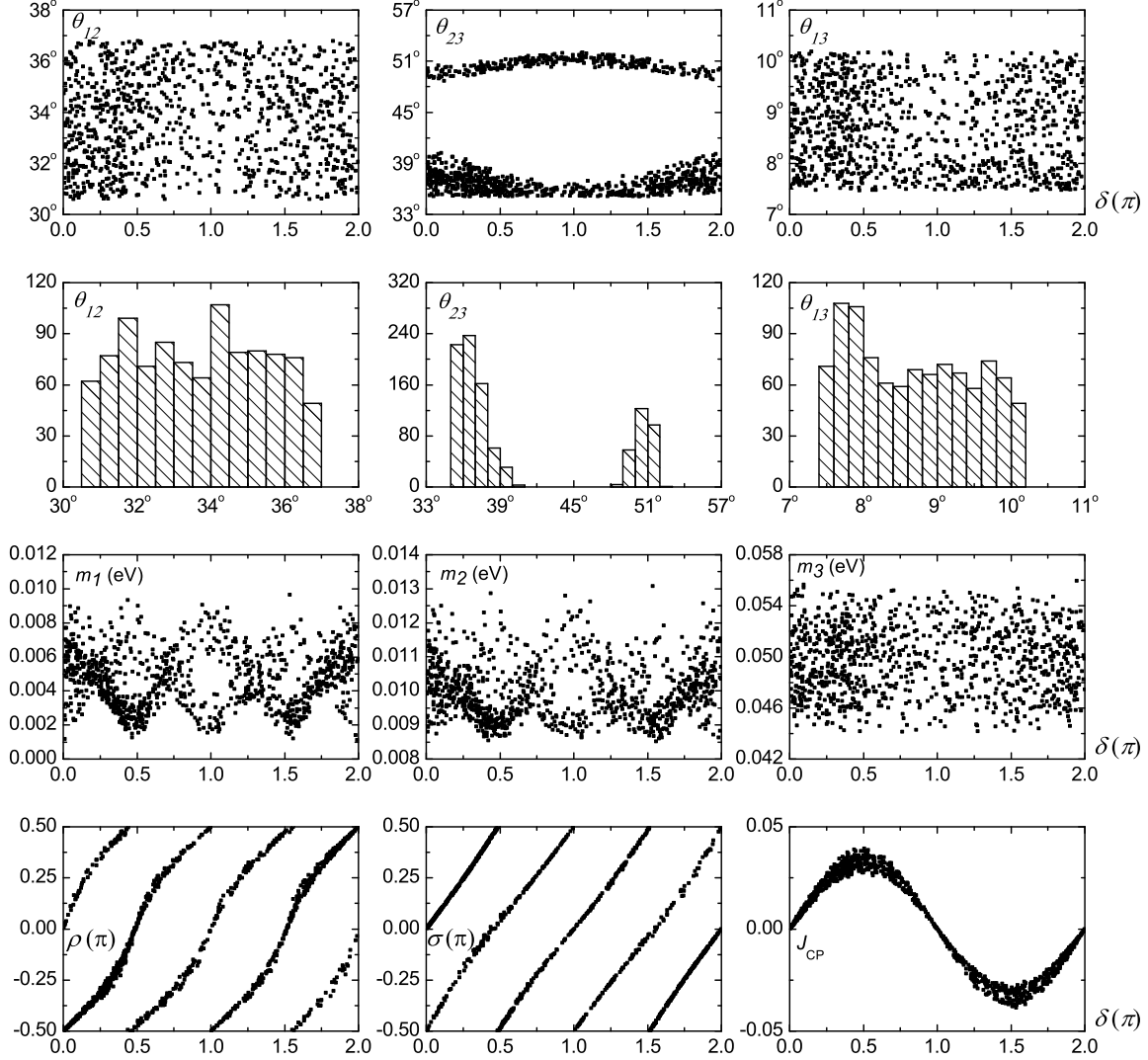


Figure 1: Pattern \mathbf{A}_1 of M_ν : The allowed ranges of flavor mixing angles ($\theta_{12}, \theta_{23}, \theta_{13}$) versus the Dirac CP-violating phase δ at the 3σ level, and the probability distribution of three angles, are given in the first and second rows, respectively. In the third and fourth rows, the predictions for three neutrino masses (m_1, m_2, m_3), the Majorana CP-violating phases (ρ, σ) and the Jarlskog invariant J_{CP} are shown with respect to the Dirac CP-violating phase δ .

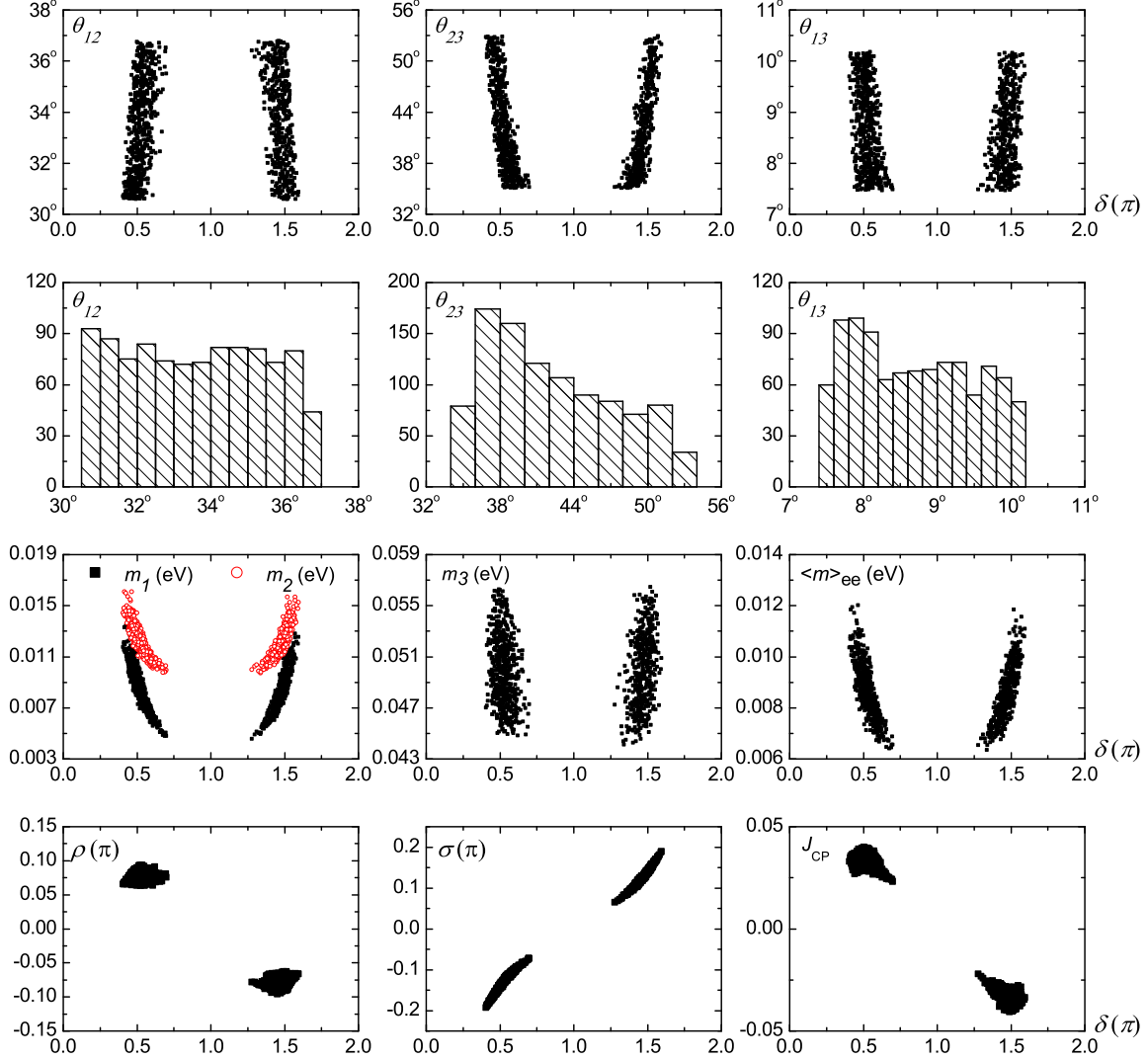


Figure 2: Pattern \mathbf{B}_1 of M_ν : The allowed ranges of flavor mixing angles ($\theta_{12}, \theta_{23}, \theta_{13}$) versus the Dirac CP-violating phase δ at the 3σ level, and the probability distribution of three angles, are given in the first and second rows, respectively. In the third and fourth rows, the predictions for three neutrino masses (m_1, m_2, m_3) and the effective neutrino mass in neutrinoless double-beta decays $\langle m \rangle_{ee}$, the Majorana CP-violating phases (ρ, σ) and the Jarlskog invariant J_{CP} , are shown with respect to the Dirac CP-violating phase δ .

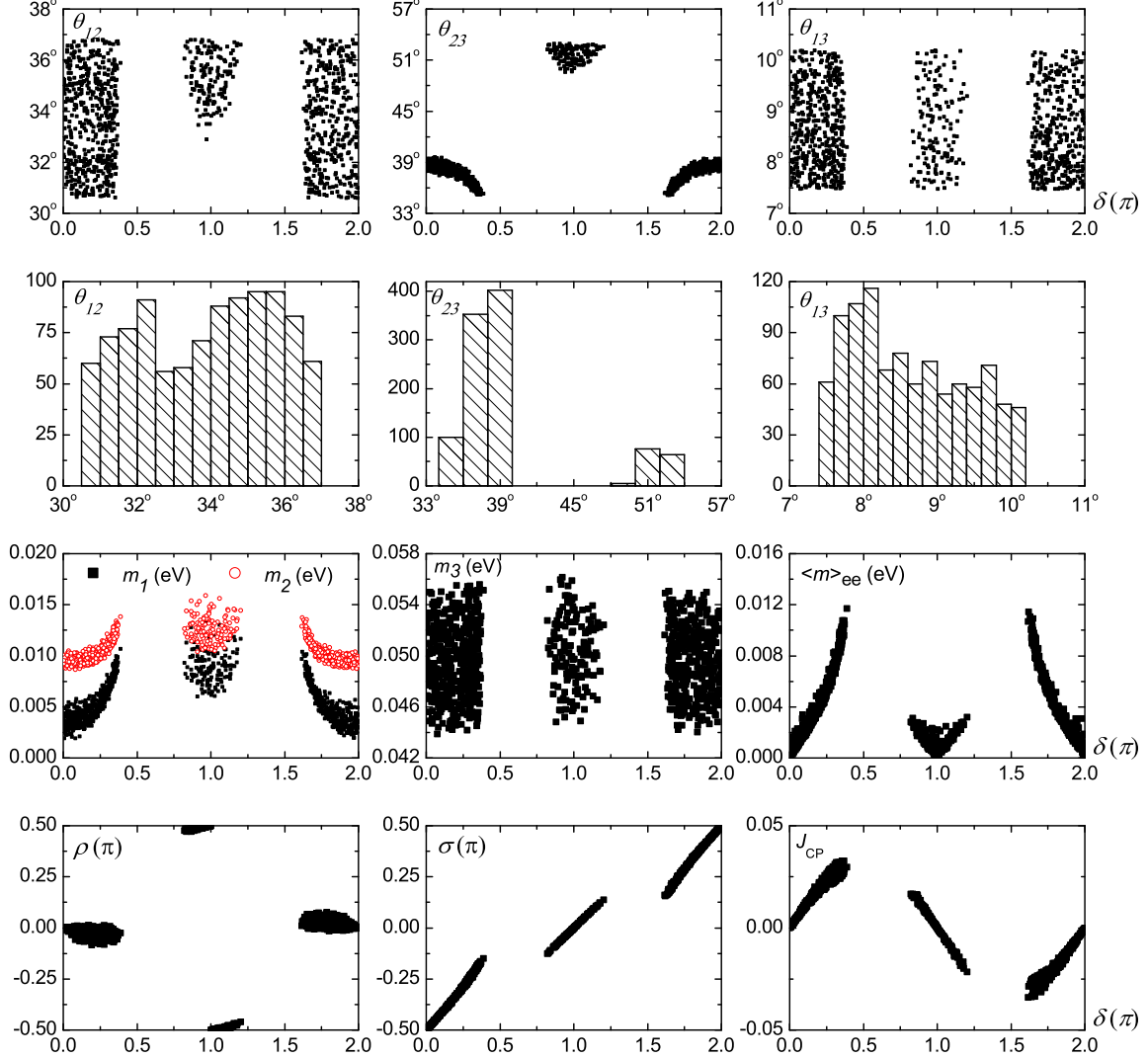


Figure 3: Pattern \mathbf{B}_5 of M_ν : The allowed ranges of flavor mixing angles ($\theta_{12}, \theta_{23}, \theta_{13}$) versus the Dirac CP-violating phase δ at the 3σ level, and the probability distribution of three angles, are given in the first and second rows, respectively. In the third and fourth rows, the predictions for three neutrino masses (m_1, m_2, m_3) and the effective neutrino mass in the neutrinoless double-beta decays $\langle m \rangle_{ee}$, the Majorana CP-violating phases (ρ, σ) and the Jarlskog invariant J_{CP} , are shown with respect to the Dirac CP-violating phase δ .

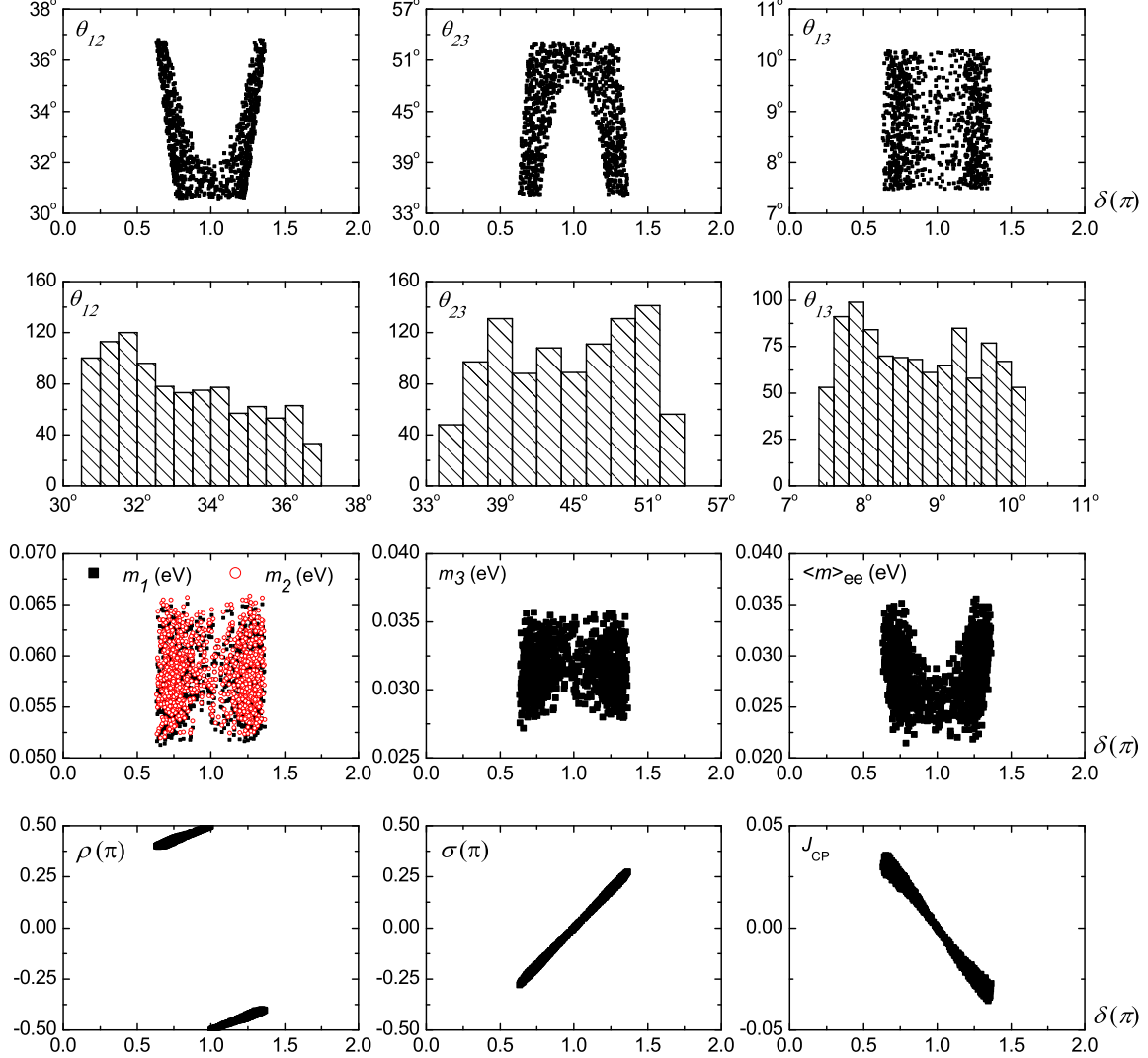
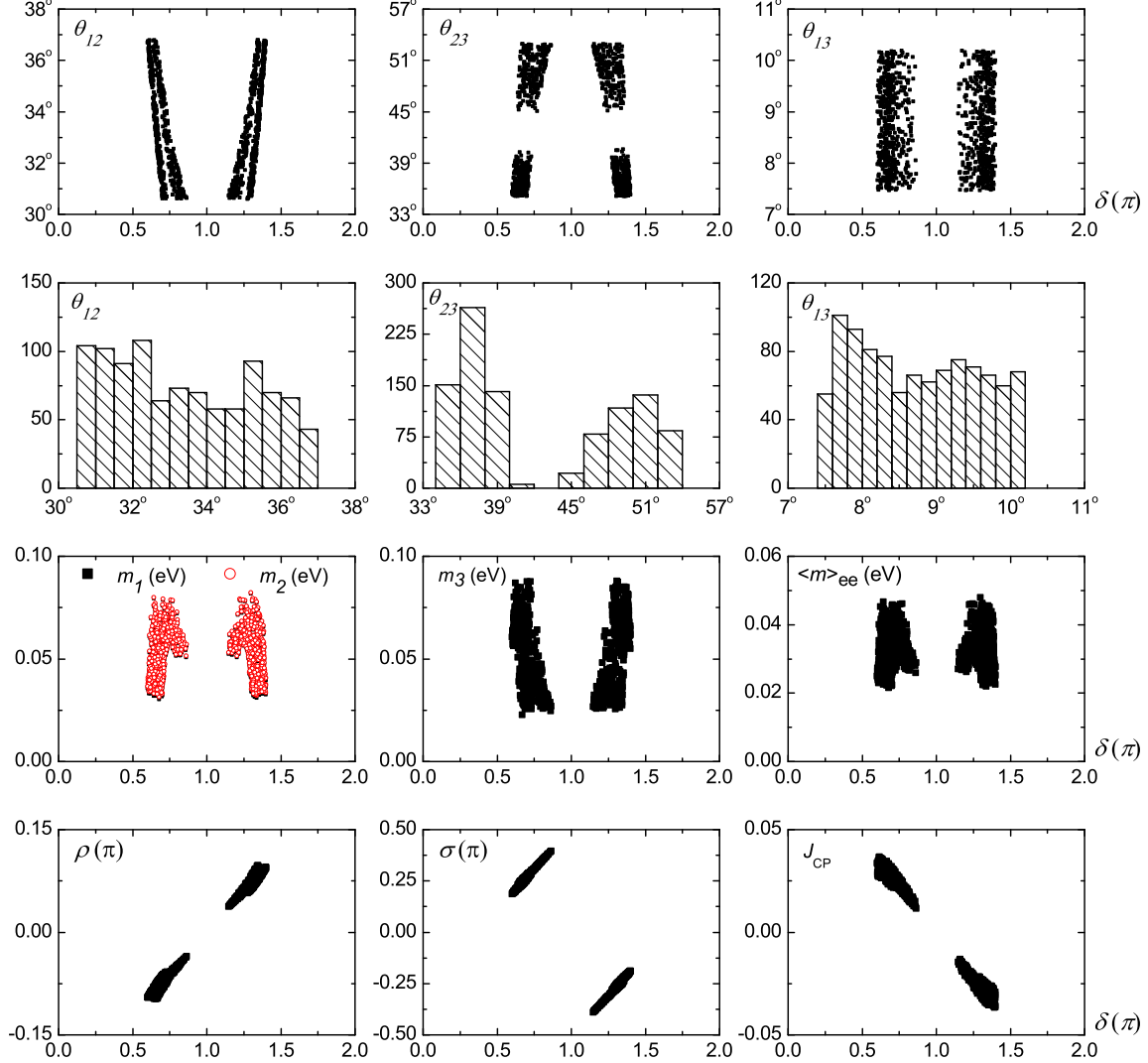


Figure 4: Pattern \mathbf{D}_1 of M_ν : The allowed ranges of flavor mixing angles ($\theta_{12}, \theta_{23}, \theta_{13}$) versus the Dirac CP-violating phase δ at the 3σ level, and the probability distribution of three angles, are given in the first and second rows, respectively. In the third and fourth rows, the predictions for three neutrino masses (m_1, m_2, m_3) and the effective neutrino mass in the neutrinoless double-beta decays $\langle m \rangle_{ee}$, the Majorana CP-violating phases (ρ, σ) and the Jarlskog invariant J_{CP} , are shown with respect to the Dirac CP-violating phase δ .



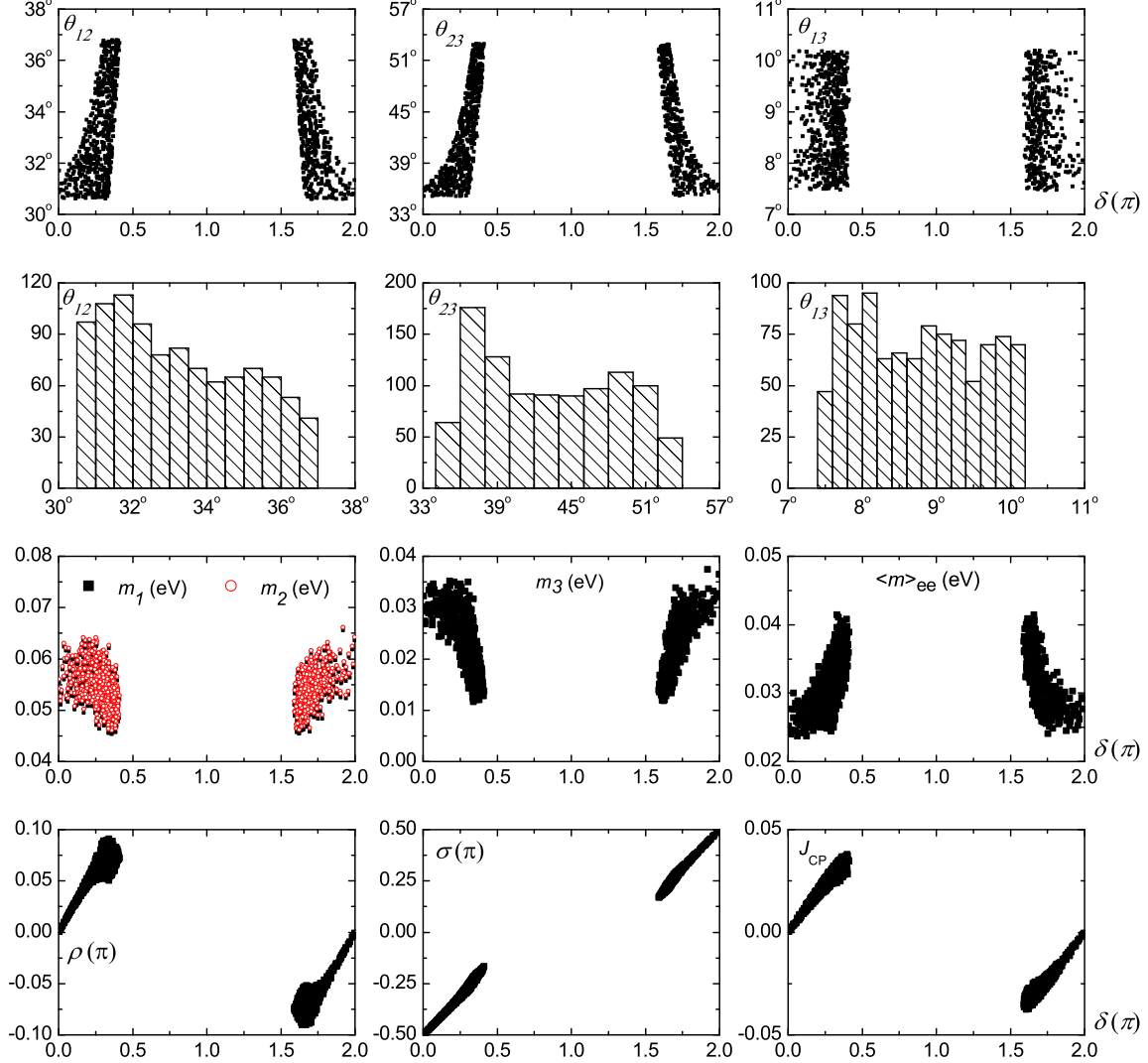


Figure 6: Pattern \mathbf{E}_8 of M_ν : The allowed ranges of flavor mixing angles ($\theta_{12}, \theta_{23}, \theta_{13}$) versus the Dirac CP-violating phase δ at the 3σ level, and the probability distribution of three angles, are given in the first and second rows, respectively. In the third and fourth rows, the predictions for three neutrino masses (m_1, m_2, m_3) and the effective neutrino mass in the neutrinoless double-beta decays $\langle m \rangle_{ee}$, the Majorana CP-violating phases (ρ, σ) and the Jarlskog invariant J_{CP} , are shown with respect to the Dirac CP-violating phase δ .